ChemPubSoc Europe

DOI: 10.1002/chem.201402519

CHEMISTRY A European Journal Full Paper

Peptidomimetics

Synthesis and Analysis of the Conformational Preferences of 5-Aminomethyloxazolidine-2,4-dione Scaffolds: First Examples of β^2- and $\beta^{2,2}$-Homo-Freidinger Lactam Analogues

Arianna Greco, Sara Tani, Rossella De Marco,* and Luca Gentilucci*[a]

Abstract: Constrained peptidomimetic scaffolds are of considerable interest for the design of therapeutically useful analogues of bioactive peptides. We present the single-step cyclization of (*S*)- or (*R*)-α-hydroxy-β^2- or α-substituted-α-hydroxy-$\beta^{2,2}$-amino acids already incorporated within oligopeptides to 5-aminomethyl-oxazolidine-2,4-dione (Amo) rings. These scaffolds can be regarded as unprecedented β^2- or $\beta^{2,2}$-homo-Freidinger lactam analogues, and can be equipped with a proteinogenic side chain at each residue. In a biomimetic environment, Amo rings act as inducers of extended, semi-bent or folded geometries, depending on the relative stereochemistry and the presence of α-substituents.

Introduction

Although native biologically active peptides have great potential for medical and biotechnological applications,[1] their utility is reduced by severe inherent limitations, in particular poor stability against proteolytic breakdown and restricted biodistribution and bioavailability.[2] Peptides also tend to be quite flexible, and conformations are highly dependent on the environment, leading to modest receptor selectivity. These issues have been addressed by the design of highly stable and conformationally constrained peptidomimetics;[1,2] that is, compounds with pharmacophoric and stereostructural elements that mimic the bioactive structure of the parent peptides.[3]

One approach to obtaining more rigid peptidomimetics[1–3] is to incorporate local constraints using conformationally restricted amino acid units or modified peptide backbones. Global constraints are introduced for instance through cyclization or by replacing portions of the peptides with nonpeptide structures. In this context, significant effort has been dedicated to the design of scaffolds that mimic turn structures. β-Turns are common motifs in peptide structures (Figure 1), and they are very often critical to peptide conformational stability, with many interactions correlated to a variety of biological processes.[3,4] Native β-turns involve four residues with Cα(*i*) to Cα(*i*+3) distances of less than 7.0 Å, and form a hydrogen-bond C=O(*i*)···H–N(*i*+4) (1↦4-type).[5] As a consequence, small scaffolds that reproduce these features have been extensively investigated to discover compounds that can mimic or disrupt turn-mediated recognition events.[6] For instance, the prototypic Freidinger lactam dipeptides[2,4,7] have been widely used to constrain peptide conformations, stabilizing turn structures and acting as strand inducers (Figure 1).[8]

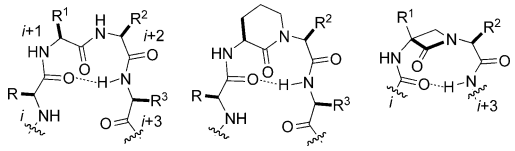

Figure 1. Sketch of a β-turn, a classic Freidinger lactam, and the α-amino-β-lactam approach.

However, the scaffold strategy has so far resulted in limited success with bioactive peptide ligands for which the nonpeptide or pseudopeptide scaffold itself contains most of the pharmacophore elements.[3,6] Frequently, the side chains at some fundamental positions are not maintained, or one of the amino acids is omitted on the basis of the hypothesis that some residues play a structural rather than a recognition role; for example, Pro or Gly at position $i+1$ of a β-turn.[6,9] Therefore, the structures of the turn mimetics may lack some relevant pharmacophores for specific targets. An example is represented by the early Freidinger lactams (Figure 1) obtained by sacrificing the $i+1$ side chain with the formation of five- to eight-membered rings. To overcome this limit, much effort has been dedicated to the preparation of α-substituted lactams;[10] for instance, Palomo et al. proposed the separation of constraint and recognition elements, and introduced α-alkyl-α-amino-β-lactam rings placed at the position $i+1$ residue as potent nucleators of β-turns (Figure 1).[11]

Furthermore, the preparation of constrained mimetics may require multistep procedures, resulting in low overall yields, and many synthetic methods lack flexibility and are therefore not suited to the introduction of diversity.[6] As a consequence, the development of an expedient procedure with which to

[a] *A. Greco, S. Tani, R. De Marco, L. Gentilucci*
Dept. of Chemistry "G. Ciamician", University of Bologna
via Selmi 2, 40126, Bologna (Italy)
Fax: (+39) 0512099456
E-mail: rossella.demarco2@unibo.it
luca.gentilucci@unibo.it

Supporting information for this article is available on the WWW under http://dx.doi.org/10.1002/chem.201402519.

constrain a peptide while maintaining all of the pharmacophores is of considerable interest.

In the last few years, we have been interested in the rapid and simple ring closure of β-hydroxy-α-amino acids into turn-inducer scaffolds. Very recently, we observed that the reaction of *N*-arylsulfonyl-peptides containing L- or D-configured Ser and/or other β-hydroxy-α-amino acids (Thr, PhSer), with *N*,*N*′-disuccinimidyl carbonate (DSC) and a catalytic amount of diisopropylethylamine (DIPEA), gave rise in a single step to the formation of oxazolidinone (Oxd) ring(s) (Scheme 1).[12] Under the same conditions, the corresponding Fmoc- or Boc-peptides gave elimination to dehydroalanine, in agreement with previous reports,[13] suggesting that the N-sulfonyl group effectively promoted the cyclization.

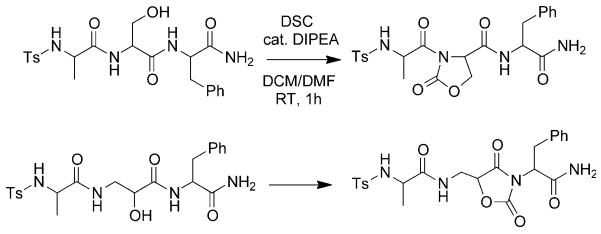

Scheme 1. Reaction of peptides containing Ser (top) or *iso*Ser (bottom) with DSC.

In this paper we describe a single-step procedure to lock the geometry of a oligopeptide by cyclization of α-hydroxy-β^2-amino acids or α-substituted-α-hydroxy-β^{2,2}-amino acids, already present in the sequence, to 5-aminomethyloxazolidine-2,4-dione rings (Amo). These unusual heterocyclic scaffolds (Scheme 1 and Figure 2) can be regarded as β^2- or β^{2,2}-homo variants of a classic Freidinger lactam and can be equipped with a side chain at each α-position.

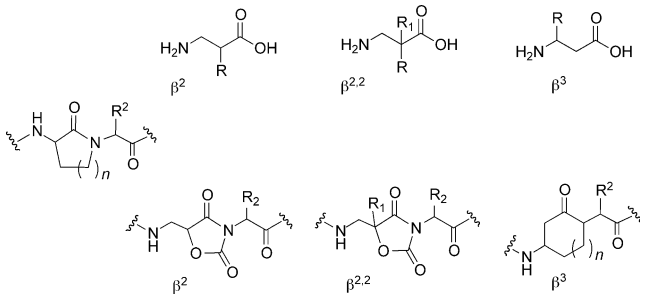

Figure 2. Structures of β^2-, β^{2,2}-, and β^3-amino acids (top), and comparison of a classic Freidinger lactam composed of all α-amino acids (middle), with the β^2- and β^{2,2}-homo Amo variants, and with a Gmeiner's β^3-homo lactams[18] (bottom).

Results and Discussion

Synthesis

On repeating the same protocol depicted in Scheme 1 with a peptide containing the α-hydroxy-β^2-amino acid isoserine (*iso*Ser) , we observed, as could have been expected, a different outcome: the reaction led exclusively to cyclization to give 5-aminomethyloxazolidine-2,4-dione (Amo) comprising *iso*Ser and the following amino acid (Scheme 1). To our knowledge, this peptide represents the first example of a conformationally constrained peptide containing an oxazolidine-2,4-dione scaffold; in general, this heterocycle has been described and utilized very few times in organic or medicinal chemistry.[14]

From a structural point of view, Amo can be regarded as a novel constrained β^2-amino acid. Among the β-amino acids, the β^2-amino acids are less synthetically feasible with respect to their β^3-counterparts (Figure 2).[15] Moreover, the cyclic structure of Amo, achieved through acylation of the backbone nitrogen atom, embraces two consecutive amino acids, therefore introducing a global constraint of C(*i*)–N(*i*+1) type[3a] in the sequence. This kind of short-range cyclization[16] can significantly reduce the conformational space accessible to the peptide segment in which they are incorporated. In this context, the Amo ring can be regarded as a novel β^2-homo analogue of a Freidinger lactam (Figure 2).[17] Structures combining the conformational properties of the Freidinger lactams with the stability of the β-amino acids have been the subject of much interest by Gmeiner and co-workers and by some other groups;[18] however, in all cases the reported structures were β^3-homo variants of Freidinger lactams (Figure 2).

Finally, the Amo-Phe sequence of Scheme 1 might also represent a constrained dipeptide unit composed of β^2 and α residues, which is of potential interest for the design of α/β-hybrid foldamers[19] showing unprecedented secondary structures (see also the Conformational Analysis Section). Indeed, unexpected conformational effects have often been observed when β^2-amino acids were present in the backbone instead of the more common β^3 residues.[15a]

This potential interest prompted us to exploit the cyclization to prepare oligopeptide sequences containing the unusual scaffold under different reaction conditions. Accordingly, we prepared a mini-library of di-, tri- or tetrapeptides containing (*S*)- or (*R*)-configured *iso*Ser, equipped with different groups at the N-terminus, and amide or ester at the C-terminus (Scheme 2), and we reacted these peptides with different carbonates or dicarbonates, either in solution (Scheme 3, Table 1) or in the solid phase (Scheme 4, Table 1).The dipeptide Boc-

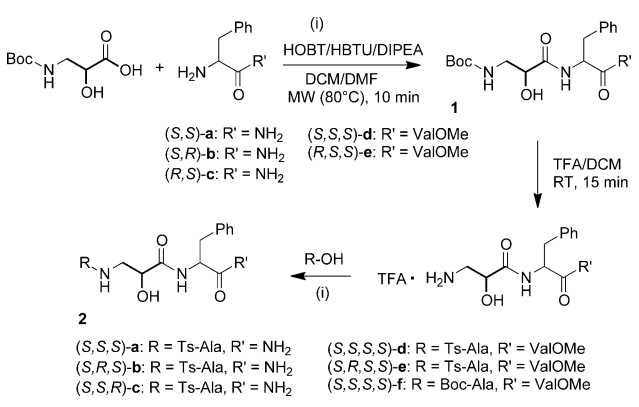

Scheme 2. Synthesis of *iso*Ser-containing peptides **1** and **2**.

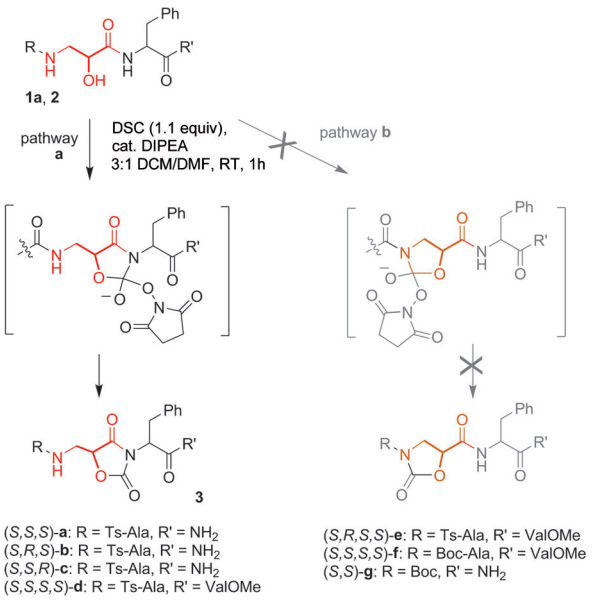

Scheme 3. Regioselective cyclization of *iso*Ser-containing peptides **1 a** and **2** to Amo-peptides **3**.

*iso*Ser-PheNH$_2$ (**1 a**) was prepared in solution by coupling Boc-*iso*SerOH and H-PheNH$_2$ under MW irradiation,[20] using HBTU/1-hydroxybenzotriazole (HOBt)/DIPEA as activating agents (Scheme 2, Step *i*). Boc-*iso*SerOH[21] was prepared according to a published procedure. The *iso*Ser building block was incorporated without protection of the OH function. Under these reaction conditions,[12] the acylation of the OH-function and thus the formation of a depsipeptide side product was not observed, as confirmed by ^{1}H NMR and RP-HPLC MS analyses of the crude reaction mixture. After purification by flash chromatography over silica gel, **1 a** was utilized for the following cyclization step (Scheme 3, Table 1).

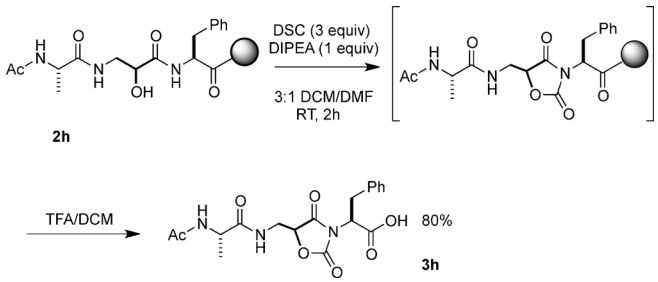

Scheme 4. Solid-phase synthesis of Ac-tripeptides **3 h**.

Table 1. Cyclization of peptides **1 a** and **2** containing *iso*Ser to Amo-peptides **3**.

Entry	1/2	R	*isoSer*	*Phe*	R′	Carbonate	3	Yield [%][a]
1	**2 a**	Ts-Ala	*S*	*S*	NH_2	DSC	**a**	93
2	**2 b**	Ts-Ala	*R*	*S*	NH_2	DSC	**b**	90
3	**2 c**	Ts-Ala	*S*	*R*	NH_2	DSC	**c**	93
4	**2 a**	Ts-Ala	*S*	*S*	NH_2	triphosgene	**a**	55
5	**2 a**	Ts-Ala	*S*	*S*	NH_2	Boc_2O	**a**	trace
6	**2 a**	Ts-Ala	*S*	*S*	NH_2	CDI	**a**	70
7	**2 d**	Ts-Ala	*S*	*S*	ValOMe	DSC	**d**	90
8	**2 e**	Ts-Ala	*R*	*S*	ValOMe	DSC	**e**	93
9	**2 f**	Boc-Ala	*S*	*S*	ValOMe	DSC	**f**	91
10	**1 a**	Boc	*S*	*S*	NH_2	DSC	**g**	91
11	**2 h**[b]	Ac-Ala	*S/R*	*S*	Phe-Wang	DSC	**h**[c]	80[d]

[a] After isolation by semipreparative RP-HPLC, see General Methods. [b] Ac-*iso*Ser-Phe-Wang resin. [c] Ac-Amo-PheOH. [d] Calculated after cleavage from the Wang resin, based on an average resin loading of 0.6 mmol g^{-1}.

By using the same protocol, Boc-*iso*SerOH and (*R*)-H-PheNH$_2$ gave **1 b**, whereas (*R*)-Boc-*iso*SerOH[21] and H-PheNH$_2$ gave **1 c**. The tripeptides **1 d** and **1 e** were prepared from Boc-*iso*SerOH and H-Phe-ValOMe (**1 d**), or (*R*)-Boc-*iso*SerOH and H-Phe-ValOMe (**1 e**). The crude compounds **1 b**–**e** were analyzed by RP-HPLC MS and utilized as intermediates for the preparation of longer sequences without further purification. The dipeptide H-Phe-ValOMe was prepared, in turn, from Boc-Phe-ValOMe,[22] by treatment with 25% trifluoroacetic acid (TFA) in dichloromethane (CH_2Cl_2). The same conditions were utilized for Boc deprotection of the di- or tripeptides **1 a**–**e** (Scheme 2).

The peptide-TFA salts from **1 a**–**e** were subjected to coupling with Tosyl (Ts)-AlaOH under the conditions described above, to give the corresponding tri- or tetrapeptides **2 a**–**e** (Scheme 2). Ts-AlaOH was prepared as described in a published procedure.[23] Finally, tetrapeptide **2 d** was obtained from **1 d** and Boc-AlaOH. The tri- or tetrapeptides **2 a**–**f** were isolated by flash chromatography over silica gel, and their structures were assigned by ^{1}H NMR and HPLC-MS analyses.

The reaction of Ts-tripeptides **2 a** and **2 b**, containing (*S*)- or (*R*)-*iso*Ser, and of the diastereoisomeric **2 c**, with DSC and DIPEA for 1 h in CH_2Cl_2/*N*,*N*-dimethylformamide (DMF) gave the corresponding Amo-peptides **3 a**–**c** with excellent yields (Scheme 3, Table 1, entries 1–3). Other carbonates or dicarbonates gave inferior results [Table 1, entry 4 (triphosgene 55%), entry 5 (Boc_2O traces), entry 6 (CDI 70%)]. Good yields were obtained with DSC for the synthesis of tetrapeptides **3 d**–**f** having Val methyl ester at the C-terminus (entries 7–9), and for the minimalist dipeptide Boc-Amo-PheNH$_2$ **3 g** (entry 10).

Different protecting groups at the N-terminus such as Boc (entries 9 and 10) and Ac (entry 11), gave results that were very similar to those obtained with Ts protection. Clearly, for the comparatively simple cleavage, carbamate protecting groups represent the most obvious choice.[24] Nevertheless, several methods have been published for the mild cleavage of arylsulfonyl groups.[24,25] Recently, we successfully removed the Ts group from peptides containing the Oxd ring with iodotrimethylsilane,[12,26] whereas treatment with SmI_2–pyrrolidine–water[27] was less efficient.

The Ac-peptide **2 h** was prepared as a mixture of diastereoisomers from racemic *iso*Ser (not protected at the OH function) by solid-phase synthesis (Scheme 4). N-Fmoc-protected amino acids were coupled on a standard Wang resin with HBTU/HOBt/DIPEA under MW irradiation (45 °C).[12] Fmoc deprotection was performed with 20% piperidine in DMF under MW irradiation. The resulting resin-bound peptide Ac-Ala-(*S*/*R*)-*iso*Ser-Phe-Wang was then utilized for the following cyclization

prior to cleavage by treatment with a moderate excess of DSC (3 equiv) and DIPEA (1 equiv) in 4:1 CH_2Cl_2/DMF for 2 h. Cleavage from resin was performed with TFA in CH_2Cl_2 in the presence of scavengers.

Analysis of the crude reaction mixture by RP-HPLC and ESI-MS revealed the presence of the two diastereomeric Amo-peptide acids Ac-Ala-(*S*/*R*)-Amo-PheOH (**3h**) in 1:1 ratio, which were recovered in very satisfactory yield (80%, based on an average resin loading of 0.6 mmol g^{-1}) after semipreparative RP-HPLC (General Methods).

In all cases, epimerization during the cyclization of **2a**–**h** was excluded on the basis of the NMR and HPLC analyses, including HPLC analysis on a chiral stationary phase (see General Methods).

The structure of the ring-closing products **3** was readily determined by ^{1}H NMR and gCOSY analyses. The disappearance of the PheNH resonance in the ^{1}H NMR spectrum, a significant downfield shift of PheHα, and the loss of the PheHα-PheNH coupling constant, established the acylation of the adjacent Phe nitrogen. In contrast, the proton pattern of the *iso*Ser residue was maintained (apart from the OH group), and the resonances of the Ala residue were practically unaffected.

In principle, the cyclization of the *iso*Ser residue with DSC could also give rise to the formation of an oxazolidin-2-one (Oxd) ring (Scheme 3, Path b); this was obtained as the only product in peptides containing Ser (Scheme 1) or other β-hydroxy-α-amino acids. The concomitant formation of traces of oxazolidinones by alternative cyclization was excluded on the basis of the HPLC, MS, and ^{1}H NMR analyses of the crude reaction mixtures. Apparently, all reactions of **2a**–**h** proceeded with complete regioselectivity, giving the Amo ring exclusively. This observation prompted us to verify whether the ring closure to Oxd occurred when the former was prevented by choosing sarcosine (Sar, *N*-methylglycine), as the *C*-terminal amino acid. Consequently, we synthesized the tripeptide Ts-Ala-*iso*Ser-SarNH$_2$ (**2i**), and attempted the cyclization reaction under the same conditions as before (Scheme 5). In effect,

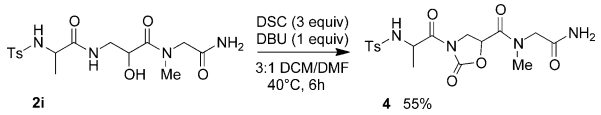

2i **4** 55%

Scheme 5. Reaction of sarcosine-containing **2i** to Oxd-peptide **4**.

after 1 h, cyclization to the corresponding peptide Ts-Ala-Oxd-SarNH$_2$ (**4**) was observed, albeit in low yield (25%) compared with that obtained with the Amo-peptides **3**, the rest being the intermediate *iso*Ser-*O*-carbonate. The yield was improved to 55% by using 1,8-diazabicyclo[5.4.0]undec-7-ene (DBU; 1 equiv) instead of catalytic DIPEA, an excess of DSC (3 equiv), higher temperatures (40 °C), and prolonged reaction times (6 h). Apparently, the cyclization to Amo **3** seems to be favored over the alternative cyclization to Oxd **4**.

Presumably, cyclization to Amo proceeds through the five-membered anionic intermediate with endocyclic C=O (Scheme 3, Path **a**, and the Supporting Information). The loss of 2,5-dioxopyrrolidin-1-olate leaving group, rapidly protonated by DIPEAH$^+$, leads to Amo-peptide **3** and DIPEA (which can be utilized in a catalytic amount). A detailed study of the reaction mechanism is beyond the scope of this work. Preliminary computations (see the Supporting Information) suggested that the intermediate with endocyclic C=O is significantly more stable than the alternative intermediate with exocyclic C=O (Scheme 3, Path b), precursor of the Oxd.

The Amo ring proved to be remarkably stable when dissolved in common organic solvents and in water. On the other hand, it has been reported that the carbamate increased the reactivity of the inner peptide bond towards reduction by $NaBH_4$.[14] Accordingly, **3b** was regioselectively reduced at the 4-position of the five-membered ring in very satisfactory yield, giving exclusively 4-hydroxy-5-aminomethyl oxazolidin-2-one **5** in *trans* relative stereochemistry (Scheme 6).

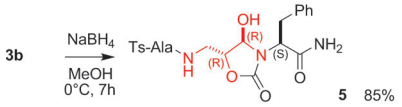

Scheme 6. Regio and stereoselective reduction of the Amo ring.

The *trans*-relationships between the two substituents was substantiated by the very small *J*(H4,H5) coupling constant in the ^{1}H NMR spectrum. 4,5-Disubstituted *trans*-oxazolidin-2-ones are characterized by coupling constants that are much lower than those of the *cis*-stereoisomers[28] (equilibrium between anomers was not observed).

Ring closure to the Amo ring was made possible by sacrificing the OH group of the α-hydroxy-β^2-amino acid *iso*Ser. Therefore, Amo represents a constrained β^2-amino acid deprived of a side chain.[15] For this reason, we exploited the opportunity to utilize α-substituted-α-hydroxy-$\beta^{2,2}$-amino acids for the preparation of Amo-derivatives carrying an explicit proteinogenic side chain. The *iso*Ser derivatives are interesting members of the β^2-amino acid family that are present in many bioactive compounds, for example, Taxol, bestatin, protease inhibitors; therefore, several synthetic protocols have been developed for their synthesis in optically active form, including asymmetric catalysis, enzymatic resolution, and the use of chiral auxiliaries and building blocks.[15,29]

As a prototype for a side chain substituted amino acid surrogate, we prepared the model nonracemic (*S*)- or (*R*)-α-methyl-*iso*Ser from a keto ester and nitromethane, using an adaptation of the catalytic enantioselective Henry reaction reported by Jørgensen (Scheme 7).[30] Methyl pyruvate was reacted with nitromethane in the presence of Cu^{II}, TEA, and (*R*)- or (*S*)-*t*Bu-bisoxazoline (Box), giving high yields of (*S*)- or (*R*)-configured β-nitro-α-hydroxy ester **6a** or **6b**, respectively.[31] Reduction of the nitro group gave the (*S*)- or (*R*)-$\beta^{2,2}$-amino ester **7a**[32] or **7b**, and coupling with the other residues under MW irradiation and standard coupling agents gave the linear homochiral tetra-

peptide **9a** or heterochiral **9b**, respectively. Treatment with DSC and base afforded the $\beta^{2,2}$-homo-Freidinger lactam analogues **10a** and **10b**, respectively, bearing a substituent at each α-position, Scheme 7.

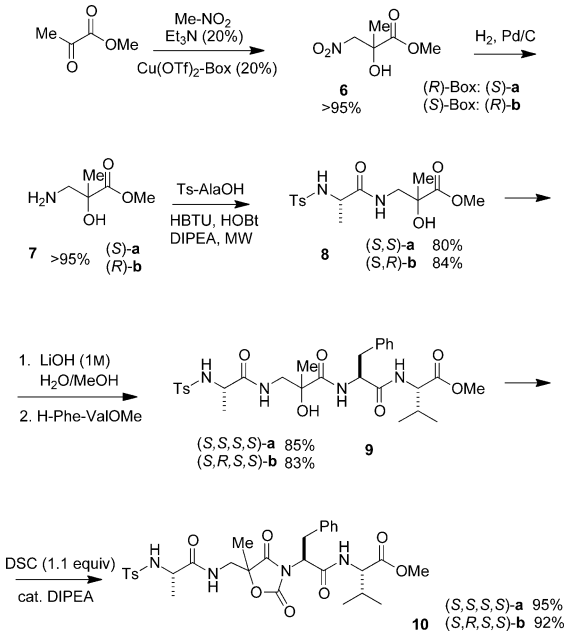

Scheme 7. Synthesis of peptides **10** containing the (*S*)- or (*R*)-configured 5-methylAmo scaffold.

Conformational analysis

For the novelty represented by the Amo scaffolds, which incorporate (*S*)- or (*R*)-β^2- or a $\beta^{2,2}$-amino acid, we decided to investigate the conformations of the Amo-containing tetrapeptides. Indeed, it is well known that the introduction of a β^2-residue in a peptide sequence can lead to secondary structures that are quite different from that of sequences composed of all α-residues.[15,19,33]

Hofmann et al. have investigated, by systematic theoretical analyses, the intrinsic conformational preferences of Ac-β-amino amide monomers carrying single or multiple substitutions at the Cα and Cβ backbone atoms. The most stable conformations were found to be different types of six- and eight-membered ring hydrogen-bonded structures (C6, C8) corresponding to gauche rotamers around the Cα–Cβ bond, which is a feature that is expected to promote local folding when incorporated into peptides.[33d,i]

In a similar way, initially we performed theoretical studies to analyze the conformational preferences of representative models of unsubstituted and α-substituted Amo monomers that we identified in the structures Ac-3-methylAmo (**11a**) and Ac-3,5-dimethylAmo (**11b**). According to the convention of Banerjee and Balaram,[33a] the soft torsional degrees of freedom in a β-amino acid are defined as ϕ (N-Cβ), θ (Cβ-Cα), and ψ (Cα-C=O), respectively (Figure 3). It is apparent that the central torsion angle θ represents the most relevant geometric variable of Amo monomers.

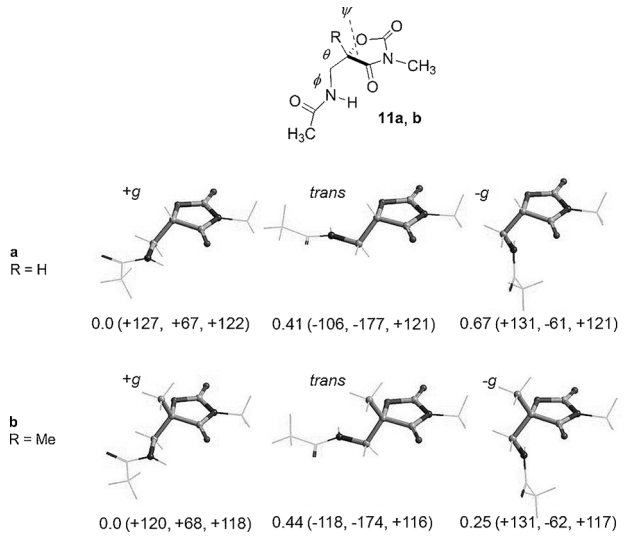

Figure 3. Minimum-energy conformations and relative energies of the $+g$, *trans*, and $-g$ rotamers around the central backbone dihedral angle θ of model compounds **11a** and **11b**. A systematic conformational analysis around ϕ and θ was performed in the gas-phase employing DFT; ΔE are given in kcal mol^{-1}; ϕ, θ, and ψ, are given in parentheses in degrees; Amo is rendered in balls and cylinders, the rest in sticks.

The relative energies of the minimum-energy conformations of the $+g$, *trans*, and $-g$ rotamers around angle θ of **11a** and **11b** have been estimated for the gas phase with the aid of theoretical studies,[34] employing the density functional theory. The calculated relative energies in increasing order were: for **11a**, $+g$ < *trans* < $-g$; for **11b**, $+g$ < $-g$ < *trans* (Figure 3). For both structures, the global minimum was a $+g$ conformer of θ, which is consistent with the calculated geometries previously reported for β^2- and disubstituted $\beta^{2,2}$-amino acids, although the rigid angle ψ prevents the formation of the commonly observed six-membered hydrogen-bonded pseudocycles (C6).[33] For **11a**, the $-g$ conformer was by far the less stable. In contrast, the presence of the methyl substituent at the 5-position of the Amo ring in **11b** strongly reduced the ΔE between the $+g$ global minimum and the $-g$ rotamer, whereas the ΔE of the *trans* geometry was slightly higher (Figure 3).

It is plausible that the geometric preferences of the Amo monomers could impact the conformations of Amo-containing oligopeptides. The computations indicated that the introduction of bulk at the α position of the scaffold should increase the population of folded structures compared with unsubstituted Amo (Figure 3) because in the former the more extended *trans* rotamer was the least stable. It is likely that when α-substituted Amo scaffold **11b** is inserted into a peptide, the preponderance of $+g$ and $-g$ rotamers should further stabilize folded geometries by intramolecular hydrogen-bonding. In oligomers, the occurrence of inter-residue hydrogen bonds or other interactions between monomers may significantly influence the stability relationships between competing alternatives, although they are not the main driving force for the formation of the corresponding conformers themselves.[19,33] Furthermore, polar solvents are expected to have an influence on the stability and conformation of molecules, and generally tend to reduce the ΔE between conformers.[33]

To experimentally determine the conformations of oligomers containing the Amo scaffolds, we performed a conformational analysis by NMR spectroscopy of the model tetrapeptides **3d** and **3e**, which include the unsubstituted (*S*)- or (*R*)-configured Amo scaffold, respectively, and **10a** and **10b** containing (*S*)- or (*R*)-5-methylAmo. To gain more information, analyses were also performed on other Amo-peptides. The ^{1}H NMR of the model compounds were recorded either in $CDCl_3$ or in 8:2 mixtures of [D_6]dimethyl sulfoxide (DMSO) and H_2O; such mixed solvent systems have been recommended by several authors as excellent representatives of biological fluids.[35] The spectra showed a single set of resonances, suggestive of conformational homogeneity or a rapid equilibrium between conformers.

In 100% $CDCl_3$, amide protons that are hydrogen bonded are found downfield with respect to nonbonded protons. For all Amo-oligopeptides, the chemical shifts of the amide protons appeared in the order AmoNH > ValNH > AlaNH. In particular, the all-(*S*)-sequences **3d** and **10a** showed AmoNH resonances above 7.0 ppm, suggesting that these amide proton were bonded to a significant extent.

The occurrence of intramolecular hydrogen-bonding was deduced by analyzing the variations of the NH chemical shifts upon addition of increasing percentages of [D_6]DMSO to solutions of the compounds in $CDCl_3$ (Figure 4).

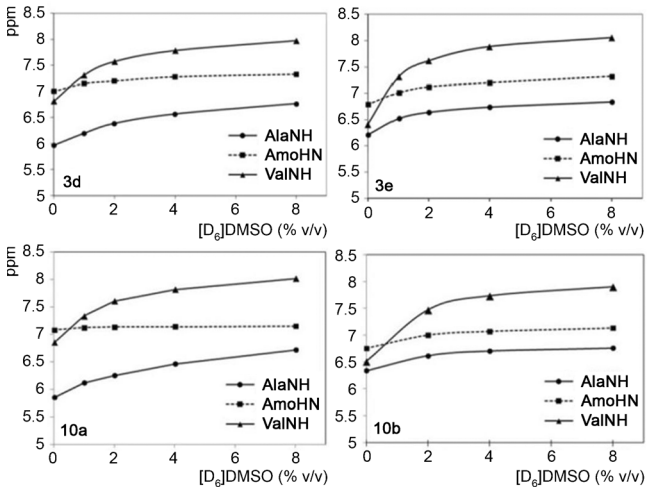

Figure 4. Variation of NH proton chemical shift (ppm) of 2 mM **3d**, **3e**, **10a**, and **10b** in $CDCl_3$ as a function of increasing [D_6]DMSO (% v/v).

During the titration of **3e** and **10b**, AlaNH and AmoNH exhibited a moderate downfield shift, whereas ValNH was much more sensitive. For **3d**, AmoNH was significantly less sensitive than AlaNH and ValNH. In contrast, for **10a**, the chemical shifts of AlaNH and ValNH showed a marked variation, whereas that of AmoNH remained practically constant and was therefore less accessible. This suggested that AmoNH could be involved in a H-bond in **10a**.[36]

To gain more information, tripeptides **3a** and **3c** were analyzed by titration experiments (see the Supporting Information). They both behaved in similar ways to tetrapeptides **3d** and **10a**, namely showing that AmoNH was possibly involved in a hydrogen bond; this observation reasonably excludes ValOMe as H-bond acceptor in the tetrapeptides. The reversal of configuration of residue 3, from (*S*) in **3a** to (*R*) in **3c**, also seemed to be well tolerated.

Variable-temperature (VT) NMR experiments were used to detect if amide protons were involved in intramolecular hydrogen-bonding or are solvent exposed. The analyses were performed in $CDCl_3$ and 8:2 mixture of [D_6]DMSO/H_2O (Table 2). In

Table 2. $\Delta\delta/\Delta t$ values (p.p.b./K) for the amide protons of **3d**, **3e**, **10a**, **10b**, in $CDCl_3$ or 8:2 [D_6]DMSO/H_2O.

Compd	Solvent	AlaNH	AmoNH	ValNH
3d	$CDCl_3$	−5.1	−4.9	−2.9
	[D_6]DMSO/H_2O[a]	−7.0	−6.3	−4.5
3e	$CDCl_3$	−7.0	−4.0	−0.5
	[D_6]DMSO/H_2O[a]	−7.0	−6.6	−5.0
10a	$CDCl_3$	−4.2	−4.1	−2.4
	[D_6]DMSO/H_2O[a]	−6.8	−2.1	−4.7
10b	$CDCl_3$	−6.7	−3.9	−1.0
	[D_6]DMSO/H_2O[a]	−7.1	−5.8	−4.5

[a] Ratio 8:2.

$CDCl_3$, **3e** and **10b** showed comparatively low $\Delta\delta/\Delta t$ values for ValNH with respect to AlaNH and AmoNH (for **3e**, $\Delta\delta/\Delta t = -0.5$ ppb/K; for **10b**, $\Delta\delta/\Delta t = -1.0$ ppb/K),[37] suggestive of a preference for conformations having hydrogen bonded ValNH ($|\Delta\delta/\Delta t|$ less than or close to 2.0 ppb/K). For **3d** and **10a**, the $\Delta\delta/\Delta t$ parameters in $CDCl_3$ did not allow clear deductions to be made. In [D_6]DMSO/H_2O, the $\Delta\delta/\Delta t$ parameters of **3d**, **3e**, and **10b** did not reveal any H-bonded amide proton. In contrast, the chemical shift of AmoNH for **10a** was significantly less sensitive to increasing temperature ($\Delta\delta/\Delta t$ in [D_6]DMSO/$H_2O = -2.1$ ppb/K), indicating a plausible conformation having this amide proton involved in a hydrogen bond.

The model compounds were analyzed by 2D-ROESY. In $CDCl_3$ the spectra displayed a modest number of inter-residue cross-peaks (not shown), which was indicative of conformational freedom. In contrast, in the biomimetic [D_6]DMSO/H_2O (8:2) mixed solvent the spectra were much clearer, and revealed meaningful inter-residue cross-peaks. For the experimental details and all results, see the following paragraphs.

Very often, changes in solvent composition cause meaningful changes in the shape of the peptides. Generally, apolar solvents such as chloroform are expected to increase hydrogen bonding, due to the absence of competitive solvation of donors and acceptors by individual solvent molecules.[19,36–38] Apparently, for the Amo-tetrapeptides, VT NMR and titration experiments in chloroform differently supported the possible existence or not of hydrogen bonds, accounting for a scarce conformational definition. This behavior was investigated and confirmed by means of FTIR spectroscopy and electronic circular dichroism (ECD) in a noncompetitive solvent (CH_2Cl_2).

FTIR spectroscopy in CH_2Cl_2 was utilized to analyze the amide stretching regions. Normally, nonbonded amide protons show a peak above 3400 cm^{-1}, whereas bonded amide NH ex-

hibit a peak below 3400 cm^{-1}.[39] The spectra of each tetrapeptide showed a peak above 3400 cm^{-1} and one or more peaks below 3400 cm^{-1} (see the Supporting Information), indicative of equilibria between nonbonded and multiply bonded structures.

ECD is a widely used technique for studying protein and peptide conformations. This technique is intrinsically a low-resolution method; however, it can furnish qualitative information on the presence of ordered secondary structures, although not too many examples on short peptides are reported.[40] ECD spectra of the model tetrapeptides in CH_2Cl_2 (see the Supporting Information) showed a smooth, negative band centered at approximately 240 nm. This observation could be compatible with the occurrence of nonclassical β-turns, because the n-π* band of the latter generally appear near 225 nm.[40]

On the one hand, the results of the various experiments in noncompetitive environments could reflect the existence of equilibria between diverse hydrogen bonded and nonbonded structures, as well as distorted or weak intra-residue hydrogen bonds, which can be observed in peptides composed of α- and β-residues.[19,33,41] On the other hand, in DMSO/water mixture, the analyses suggested higher conformational homogeneity. It has been demonstrated that cryoprotective mixtures of high viscosities, such as DMSO/water, showed a remarkable ability to favor compact structures representative of the bioactive conformers over disordered structures.[35,42]

As anticipated, the 2D-ROESY of the model compounds in $[D_6]$DMSO/H_2O (8:2) mixture gave analyzable cross-peaks. Compared with tetrapeptides **3e** and **10b** (not shown), the homochiral **3d** and **10a** showed a larger number of short-range inter-residue proton–proton correlations (Figure 5). In particular, **10a** also displayed several short-range cross-peaks between remote residues (for the complete list of cross-peaks, see the Supporting Information), which was suggestive of a folded structure.

Cross-peak intensities were ranked to infer plausible interproton distances as restraints (see the Supporting Information). Structures (50) consistent with ROESY were obtained by simulated annealing with restrained molecular dynamics (MD) in a box of explicit TIP3P equilibrated water molecules. With the exception of Amo-Phe, the ω bonds were set at 180°; indeed, it is well established that peptides comprising only secondary amide bonds adopt all-*trans* conformations.[43] In any case, the absence of Hα(*i*)–Hα(*i*+1) cross-peaks reasonably excluded the occurrence of *cis* peptide bonds.[44] The structures were minimized with the AMBER force field[45] and clustered by the rmsd analysis of backbone atoms. For each peptide, this procedure essentially gave one major cluster comprising the large majority of the structures. The representative structures of **3d**, **3e**, **10a**, and **10b**, with the lowest energy, were selected and analyzed (Figure 6).

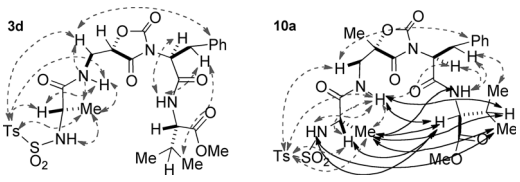

Figure 5. Sketches of the structures of **3d** and **10a**, and short-range (distances ≤3 Å) proton–proton ROESY correlations, indicated by arrows. Intraresidue and long-range (>3 Å) correlations are not shown. Grey dashed arrows connect protons belonging to consecutive residues (*i*,*i*+1), whereas black solid arrows connect protons of non-consecutive residues (*i*,*i*+2 or *i*,*i*+3).

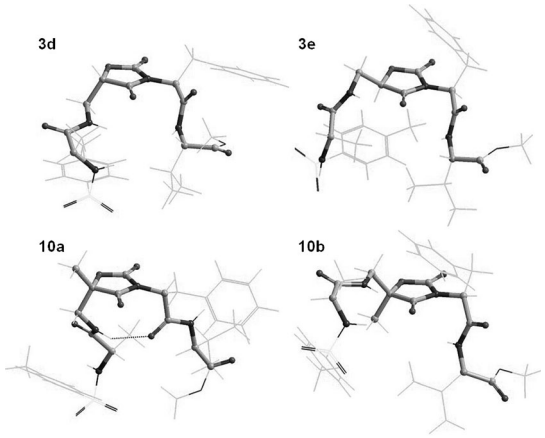

Figure 6. Representative lowest energy structures **3d**, **3e**, **10a**, and **10b**, calculated by restrained MD in a 30×30×30 Å box of standard TIP3P water molecules. Backbones and Amo rings are rendered in balls and cylinders, the rest in sticks.

In the ROESY-derived structures of the homochiral tetrapeptides **3d** and **10a**, the Ts-Ala and Val-OMe moieties occupied the same side underneath the heterocycle. The Amo residue of **3d** displayed a $+g$ conformation about the central dihedral angle ($\theta = +42°$), and a partially bent disposition of the backbone (Figure 6). In contrast, the central dihedral angle of Amo in **10a** presented a $-g$ conformation ($\theta = -53°$), and the peptide adopted a folded geometry compatible with an atypical turn centered on the dipeptide mimetic Amo-Phe. This secondary structure was stabilized by a clear 2↦1 type H-bond between AmoNH and PheC=O, in agreement with the VT NMR temperature coefficient (Table 2). The representative structure of **10a** shown in Figure 6 is characterized by the following dihedral angles (in degrees): Amo (ϕ, θ, ψ): −106, −53, −119; Phe (ϕ, ψ): +83, +143 (see also Figure 7). The distance between the amide nitrogen of Amo and the carbonyl oxygen of Phe is 3.0 Å, whereas that between AlaCα and PheCα is approximately 4.3 Å.

For tetrapeptides **3e** and **10b**, which include (*R*)-Amo scaffolds, the ROESY derived structures revealed more extended backbone conformations, with Ts-Ala and Val-OMe positioned on opposite sides of the Amo ring. For both compounds, the central dihedral angle of Amo adopted a $-g$ conformation (**3e**: $\theta = -64°$; **10b**: $\theta = -55°$). The marked differences between homo- and heterochiral peptides are not unexpected because it is well known that short sequences may experience dramatic changes of backbone conformation by reversal of the configuration of even a single residue.[2,6,11]

To analyze the dynamic behavior of the peptides, starting from the structures of Figure 6, we performed unrestrained

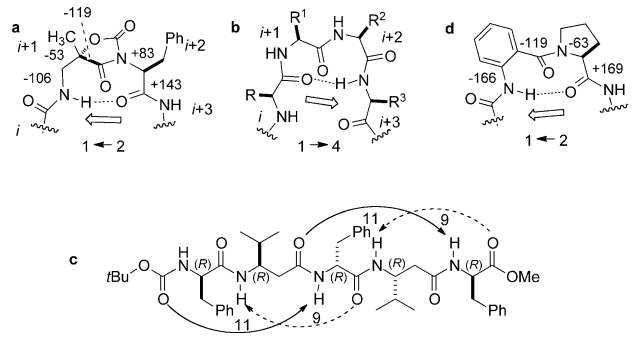

Figure 7. a) Sketch of the *pseudo* β-turn of **10a** stabilized by a nine-membered 2↦1 H-bond induced by the (*S*)-Amo scaffold, and relevant dihedral angles (deg). b) Ideal β-turn showing the ten-membered 1↦4 H-bond; c) The peptide in ref. [46]is characterized by nine-membered 2↦1 H-bonds (grey dashed arrows) as observed for **10a**, and distinct 11-membered *i*↦*i*+3 hydrogen bonds with opposite orientation; d) anthranilic acid-Pro[47] scaffold showing the nine-membered 2↦1 H-bond, and relevant dihedral angles (deg).

MD simulations for 10 ns at 300 K in a box of explicit TIP3P water molecules. For all compounds, during the simulations the complete rotation of the Phe-Val moiety around the Amo-Phe bond was not observed; possibly, the two carbonyl groups at the 2- and 4-positions of the Amo ring prevented this movement. Analyses of the trajectories of **10a** showed that the folded geometry of the backbone was maintained during the simulation, although AmoNH and PheC=O were prone to rotate about the dihedral angles Amoϕ and Pheψ, respectively, leading to occasional fluctuation of the distance PheC=*O*-Amo*N* (see the Supporting Information). Analyses of the trajectories of **3d**, **3e**, and **10b**, did not reveal the occurrence of clear secondary structures (not shown), and confirmed the higher backbone mobility of heterochiral **3e** and **10b**.

The role exerted by the residue $i+3$ on peptide conformation was not investigated. It can be expected that substitution of Phe^3 with other amino acids could modify the stability and geometry of the folded conformation.[8a,11c] It was shown that peptides incorporating a central lactam-Gly pair can exhibit high conformational heterogeneity around the lactam–Gly bond, depending on the presence and relative disposition of the substituents of the lactam scaffold.[8a,11b]

On reviewing the evidence obtained from the experimental results and theoretical computations, it can be perceived that the conformational features of **3d**, **3e**, and **10b**, seem to be governed mainly by the stereochemistry and geometric preferences of the Amo scaffold, which preferentially adopt a $+g$ orientation of the central torsion angle θ (the $-g$ conformation of (*R*)-Amo is equivalent to the $+g$ of the (*S*)-enantiomer). For **10a**, a significant population of bent conformers was expected on the basis of the higher stability of the $-g$ conformer (Figure 3), which is correlated, in turn, to the presence of the α-substituent on the Amo scaffold. This effect and the stabilization exerted by the nine-membered hydrogen bond ring appear to be the major contributors to the folding of peptide **10a**.

The conformation adopted by the model peptide **10a** in a solvent mimetic of biological fluids can be regarded as a *pseudo* β-turn, being characterized by a Cα(*i*) to Cα(*i*+3) distance of less than 7.0 Å.[47] This structure requires only the mixed β/α-dipeptide to display the closed hydrogen-bonded network (Figure 7a). The dipeptide Amo-Phe contains a nine-membered hydrogen-bonded ring between AmoNH and PheC=O of type 2↦1. This structure is in contrast to native β-turns (Figure 7b), which involve four residues to form the hydrogen-bonded structure in the opposite direction (residues 1↦4). To our knowledge, **10a** represents a very rare example of a short sequence showing this kind of *pseudo* β-turn,[48] although it was observed in linear oligomers composed of repetitive α/β-units (e.g., Figure 7c, d).

The secondary structure formed by a given type of hybrid α/β-oligomer depends on the number and type of substitution of the α- or β-residues within the units, on their stereochemistry pattern, and on conformational restraints such as the incorporation of cyclic structures within the amino acid. A variety of secondary structures have been reported, stabilized by 10- to 15-membered hydrogen-bonded rings in both orientations of the backbone direction, whereas nine-membered hydrogen-bonded rings of type 2↦1 have been described less often.[19,33]

Hofmann et al. carried out a detailed theoretical study of α/β-peptides, demonstrating the stability of a mixed helix with a nine-membered hydrogen-bond in the forward direction and an 11-membered hydrogen-bond in the backward direction of the peptide chain in apolar solvents.[33f] In contrast, the peptide Boc-[(*R*)-Phe-(*R*)-β^3-homo-Val]$_2$-(*R*)-PheOMe (Figure 7c),[46] 'heterochiral' because the β^3-residues derived from L-α-residues, was shown to adopt a mixed structure characterized by one classic 11-membered *i*↦*i*+3 hydrogen bond, and a distinct nine-membered 2↦1 hydrogen-bond with opposite orientation.[49]

More recently, the 2↦1 nine-membered hydrogen-bond ring was described by Sanjayan and Rajamohanan[47] in oligopeptide foldamers consisting of the repeating building blocks L-Pro and anthranilic acid, the latter as a rigid β-amino acid (Figure 7d). The structure was explained as the result of the combined intrinsic conformational preferences of two local constraints and the repetitive α/β-hybrid structure.[19] Replacing Pro with other residues had an adverse effect on the stabilization of this architecture. Later studies confirmed the stability of the turn motifs featuring the nine-membered hydrogen-bond ring also in tripeptides containing a distinct Ant-Pro scaffold.[48]

Remarkably, the characteristic Freidinger-lactam-like structure of the mixed β^2/α-dipeptide mimetic Amo-Phe induced **10a** to adopt, in a very competitive and biomimetic environment, a significant population of folded geometries, without the concomitant assistance of further constraint-inducers, and without the cooperative effect of repetitive units.

Conclusion

The cyclization of *iso*Ser incorporated into short peptides with DSC and DIPEA was performed either in solution or in the solid phase with very good yields, and allowed the preparation, in

a single step, of peptidomimetics containing the unusual aminomethyloxazolidin-2,4-dione (Amo) scaffold comprising *iso*Ser and the following residue. This unusual scaffold represents an unprecedented β^2-homo variant of the classic Freidinger lactam. Furthermore, the availability of optically pure α-substituted α-hydroxy-$\beta^{2,2}$-amino acids allowed the preparation of peptidomimetics carrying a single proteinogenic side chain at each residue. Conformational analyses indicated that the constrained α-substituted Amo tends to favor in homochiral oligomers a rare *pseudo* β-turn stabilized by a nine-membered hydrogen bond ring of type 2↦1 in the opposite direction of the sequence.

For the simple synthetic protocol and the atypical geometric features, the Amo ring deserves to be exploited for the design of new conformationally biased peptidomimetics or foldamers. The scope of the Amo scaffold will be extended by introducing substituents with defined stereochemistry in the β-position of the Amo motif, thus providing constrained $\beta^{2,3}$-amino acid building blocks. Further studies are in progress in our group for the preparation and analysis of the conformational preference of oligopeptides composed of repetitive Amo units, either alone or in combination with other residues.

Experimental Section

General methods

Standard chemicals [including Boc- or Fmoc-protected α-amino acids, (*S*)- and (*R*)-H-*iso*SerOH, Fmoc-*rac*-H-*iso*SerOH, (*S*)- and (*R*)-H-PheNH$_2$, H-ValOMe, H-SarNH$_2$], were purchased from commercial sources and used without further purification. Flash chromatography was performed on silica gel (230–400 mesh), using mixtures of distilled solvents. Compound purities were assessed by analytical RP-HPLC and elemental analysis. Analytical RP-HPLC was performed with an Agilent 1100 series apparatus, using a RP column [Phenomenex mod. Gemini 3μ C18 110A 100×3.0 mm (P/No 00D-4439-Y0)]; column description: stationary phase octadecyl carbon chain-bonded silica (C18) with TMS endcapping, fully porous organo-silica solid support, particle size 3 μm, pore size 110 Å, length 100 mm, internal diameter 3 mm; DAD 210 nm; mobile phase: from H_2O/CH_3CN (9:1) to a H_2O/CH_3CN (2:8) in 20 min at a flow rate of 1.0 mL min^{-1}, followed by 10 min at the same composition. Semi-preparative RP-HPLC was performed with an Agilent 1100 series apparatus, using a RP column [ZORBAX mod. Eclipse XDB-C18 PrepHT cartridge 21.2×150 mm 7μ (P/No 977150–102)]; column description: stationary phase octadecyl carbon chain-bonded silica (C18), double endcapped, particle size 7 μm, pore size 80 Å, length 150 mm, internal diameter 21.2 mm; DAD 210 nm; mobile phase from H_2O/CH_3CN (8:2) to CH_3CN (100%) in 10 min at a flow rate of 12 mL min^{-1}. Chiral HPLC analysis was performed with an Agilent 1200 series apparatus, using a CHIRALPAK IC column (P/No 83325); column description: chiral stationary phase cellulose *tris*(3,5-dichlorophenylcarbamate) immobilized on silica, particle size 5 μm, length 250 mm, internal diameter 4.6 mm, DAD 210/254 nm; mobile phase: *n*-hexane/2-propanol (3:1), at 0.8 mL min^{-1}. The RP-HPLC of compounds **3h**, H-Phe-ValOMe, **7**, and Ts-Ala-α-Me-*iso*SerOH, was performed as reported above, with the addition of 0.1% TFA in the mobile phase, and setting DAD at 254 nm. MS (ESI) analysis was performed using a MS single quadrupole HP 1100 MSD detector, with a drying gas flow of 12.5 L min^{-1}, nebulizer pressure 30 psgi, drying gas temp. 350 °C, capillary voltage 4500 (+) and 4000 (−), scan 50–2600 amu. Elemental analyses were performed with a Thermo Flash 2000 CHNS/O analyzer. High quality IR were obtained at 2 cm^{-1} resolution with an FTIR spectrometer and 1 mm NaCl solution cell. ECD spectra were recorded with a Jasco J-710 spectropolarimeter. The synthetic procedures by MW irradiation were performed with a microwave oven (Micro-SYNTH Microwave Labstation for Synthesis) equipped with a built-in ATC-FO advanced fiber optic automatic temperature control. ^{1}H NMR spectra were recorded with a Varian Gemini apparatus at 400 MHz in 5 mm tubes, using 0.01 M peptide at RT. Solvent suppression was performed by the solvent presaturation procedure implemented in Varian (PRESAT). ^{13}C NMR spectra were recorded at 100 MHz. Chemical shifts are reported as δ values relative to residual $CHCl_3$ (δ_H = 7.26 ppm), DMSO (δ_H = 2.50 ppm), and $CDCl_3$ (δ_C = 77.16 ppm) as internal standards. The unambiguous assignment of ^{1}H NMR resonances was based on 2D gCOSY experiments. VT-^{1}H NMR experiments were performed over the range of 298–348 K; temperature calibration was done with the ethylene glycol OH-CHn chemical-shift separation method.

Boc-(*S*)-*iso*Ser-(*S*)-PheNH$_2$ (1a): A stirred solution of Boc-*iso*Ser-OH (0.20 g, 1.0 mmol) in CH_2Cl_2/DMF (4:1, 5 mL) was treated with HOBt (0.16 g, 1.2 mmol) and HBTU (0.46 g, 1.2 mmol), at r.t., under a nitrogen atmosphere. After 5 min, H-PheNH$_2$ (0.18 g, 1.1 mmol) and DIPEA (0.42 mL, 2.4 mmol) were added, and the mixture was stirred under a nitrogen atmosphere under MW irradiation. The microwave-assisted reaction was performed with an initial irradiation power of 150 W, and monitoring the internal reaction temperature at 80 °C with a built-in ATC-FO advanced fiber optic automatic temperature control. After 10 min, the mixture was concentrated at reduced pressure and the residue was diluted with EtOAc (25 mL). The solution was washed with 0.1 M HCl (5 mL), and a saturated solution of $NaHCO_3$ (5 mL). The organic layer was dried over Na_2SO_4 and the solvent was evaporated at reduced pressure. Peptide **1a** was isolated (0.29 g, 80%, 91% pure by analytical RP-HPLC, see General Methods, R_t = 4.33 min) by flash chromatography over silica gel (EtOAc/MeOH, 95:5). ^{1}H NMR ($CDCl_3$): δ = 1.34 (s, 9H; *t*Bu), 3.00–3.17 (m, 2H; PheHβ), 3.20–3.36 (m, 2H; isoSerHβ), 4.10 (m, 1H; *iso*SerHα), 4.59 (q, *J* = 6.8 Hz, 1H; PheHα), 5.38 (br. t, 1H; *iso*SerNH), 6.29 (s, 1H; $CONH_2$), 6.79 (s, 1H; $CONH_2$), 7.08–7.12 (m, 3H; PheArH), 7.12–7.20 (m, 2H; PheArH), 7.61 ppm (br. d, 1H; PheNH); MS (ESI): *m/z*: 374.4 [*M*+Na]$^+$ found: 374.4.

Boc-(*S*)-*iso*Ser-(*R*)-PheNH$_2$ (1b) and Boc-(*R*)-*iso*Ser-(*S*)-PheNH$_2$ (1c): The reaction of Boc-*iso*SerOH and (*R*)-H-PheNH$_2$, or (*R*)-Boc-*iso*SerOH and H-PheNH$_2$, using the same reagent quantities and under same MW-assisted conditions described for the preparation of **1a**, afforded dipeptides **1b** or **1c**, respectively. After the same work up, crude **1b**,**c** were precipitated from MeOH/Et_2O and collected by filtration. The crude peptides were identified by MS (ESI), and purity was assessed by analytical RP-HPLC (General Methods).

Compound 1b: Yield: 86% (76% pure); R_t = 4.01 min; MS (ESI): *m/z* calcd 352.4 [*M*+1]$^+$ found: 352.2.

Compound 1c: Yield: 85% (78% pure); R_t = 3.49 min; MS (ESI): *m/z* calcd 352.4 [*M*+1]$^+$ found: 352.3.

Boc-(*S*)-*iso*Ser-(*S*)-Phe-ValOMe (1d) and Boc-(*R*)-*iso*Ser-(*S*)-Phe-ValOMe (1e): Boc-Phe-ValOMe[22] (1.13 g, 3.0 mmol) was N-deprotected according to the General Procedure for Boc Deprotection, giving H-Phe-ValOMe-TFA salt in quantitative yield (90% pure by analytical RP-HPLC, see General methods, R_t = 1.82 min), identified by MS (ESI) analysis (*m/z* calcd 279.2 [*M*+1]$^+$ found: 279.2). The crude dipeptide was coupled with Boc-*iso*SerOH or Boc-(*R*)-*iso*SerOH by using the same quantities and under same conditions described for the preparation of **1a**, affording dipeptides **1d** or **1e**,

respectively. After the same work up, crude **1 d**,**e** were analyzed by RP-HPLC ESI-MS (General Methods).

Compound 1 d: Yield: 82% (75% pure); R_t = 4.30 min; MS (ESI): *m/z* calcd 466.2 $[M+1]^+$ found: 466.1.

Compound 1 e: Yield: 80% (73% pure); R_t = 4.62 min; MS (ESI): *m/z* calcd $[M+1]^+$ 466.2 found: 466.2.

General procedure for Boc deprotection

The intermediate N-Boc peptides **1** (1.0 mmol) were deprotected by treatment with 25% TFA in CH_2Cl_2 (5 mL) while stirring at r.t. After 15 min, the solution was evaporated under reduced pressure, and the treatment was repeated. The residue was suspended in ice-cold Et_2O (20 mL). The intermediate peptide-TFA salts, which precipitated in almost quantitative yields, were collected by centrifuge, and used for the next couplings without further purification (80–85% pure by analytical RP-HPLC, General Methods).

General procedure for the synthesis of peptides 2 e–f

The N-deprotected peptide-TFA salts prepared from peptides **1** as described above were subjected to coupling with Tosyl (Ts)-AlaOH or Boc-AlaOH in the same scale by using the same procedure utilized for **1 a**, giving the corresponding tri- or terapeptides **2 a**–**e** or **2 f**, respectively. After the usual workup, the peptides were isolated (80–85%) by flash chromatography over silica gel (EtOAc/MeOH, 95:5).

Ts-(*S*)-Ala-(*S*)-*iso*Ser-(*S*)-PheNH$_2$ (2 a): 90% pure by RP-HPLC (General Methods); R_t = 4.86 min; ^{1}H NMR ($CDCl_3$): δ = 1.00 (d, *J* = 6.8 Hz, 3H; AlaMe), 2.37 (s, 3H; TsMe), 2.71 (ddd, *J* = 5.0, 8.2, 13.8 Hz, 1H; *iso*SerHβ), 2.88 (dd, *J* = 7.8, 13.8 Hz, 1H; PheHβ), 3.02 (dd, *J* = 5.0, 13.8 Hz, 1H; PheHβ), 3.20 (ddd, *J* = 4.4, 6.2, 13.8 Hz, 1H; *iso*SerHβ), 3.73 (dq, *J* = 5.2, 6.8 Hz, 1H; AlaHα), 3.79 (dd, *J* = 4.4, 8.2 Hz, 1H; *iso*SerHα), 4.49 (ddd, *J* = 5.0, 5.6, 7.8, 1H; PheHα), 5.86 (d, *J* = 5.2 Hz, 1H; AlaNH), 7.16–7.27 (m, 5H; PheArH), 7.35 (m, 2H; $TsArH_{3,5}$), 7.51 (s, 1H; $CONH_2$), 7.63–7.69 (m, 3H; $TsArH_{2,6}$ and PheNH), 7.77 (dd, *J* = 5.0, 6.2 Hz, 1H; *iso*SerNH), 7.86 ppm (s, 1H; $CONH_2$); MS (ESI): *m/z* calcd 477.2 $[M+H]^+$ found: 477.4.

Ts-(*S*)-Ala-(*R*)-*iso*Ser-(*S*)-PheNH$_2$ (2 b): 88% pure by RP-HPLC (General Methods); R_t = 4.16 min; ^{1}H NMR ($CDCl_3$): δ = 0.99 (d, *J* = 6.8 Hz, 3H; AlaMe), 2.36 (s, 3H; TsMe), 2.86–2.98 (m, 2H; *iso*SerHβ and PheHβ), 3.01 (dd, *J* = 4.8, 13.9 Hz, 1H; PheHβ), 3.22 (ddd, *J* = 4.6, 6.2, 13.8 Hz, 1H; *iso*SerHβ), 3.74 (dq, *J* = 5.0, 6.8 Hz, 1H; AlaHα), 3.78 (dd, *J* = 4.6, 8.0 Hz, 1H; *iso*SerHα), 4.46 (ddd, *J* = 4.8, 5.7, 7.6 Hz, 1H; PheHα), 5.79 (d, *J* = 5.0 Hz, 1H; AlaNH), 7.16–7.27 (m, 5H; PheArH), 7.35 (m, 2H; $TsArH_{3,5}$), 7.51 (s, 1H; $CONH_2$), 7.64–7.67 (m, 3H; $TsArH_{2,6}$ and PheNH), 7.75 (dd, *J* = 4.8, 6.2 Hz, 1H; *iso*SerNH), 7.85 ppm (s,1H; $CONH_2$); MS (ESI): *m/z* calcd 477.2 $[M+H]^+$ found: 477.4.

Ts-(*S*)-Ala-(*S*)-*iso*Ser-(*R*)-PheNH$_2$ (2 c): 91% pure by RP-HPLC (General Methods); R_t = 4.45 min; ^{1}H NMR ($CDCl_3$): δ = 1.18 (d, *J* = 7.0 Hz, 3H; AlaMe), 2.42 (s, 3H; TsMe), 3.04 (dd, *J* = 8.2, 14.0 Hz, 1H; PheHβ), 3.23 (dd, *J* = 6.0, 14.0 Hz, 1H; PheHβ), 3.63 (ddd, *J* = 4.8, 8.2, 13.8 Hz, 1H; *iso*SerHβ), 3.68–3.78 (m, 2H; AlaHα and *iso*SerHβ), 4.16 (m, 1H; *iso*SerHα), 4.49 (dd, *J* = 6.0, 6.4, 8.2 Hz, 1H; PheHα), 5.32 (d, *J* = 2.4 Hz, 1H; *iso*SerOH), 5.93 (d, *J* = 7.6 Hz, 1H; AlaNH), 6.34 (s, 1H; $CONH_2$), 6.79 (s, 1H; $CONH_2$), 7.18–7.31 (m, 7H; $TsArH_{3,5}$ and PheArH), 7.61 (d, *J* = 6.4 Hz, 1H; PheNH), 7.68 (dd, *J* = 4.8, 6.0 Hz, 1H; *iso*SerNH), 7.75 ppm (m, 2H; $TsArH_{2,6}$); MS (ESI): *m/z* 477.4.

Ts-(*S*)-Ala-(*S*)-*iso*Ser-(*S*)-Phe-(*S*)-ValOMe (2 d): 89% pure by RP-HPLC (General Methods); R_t = 4.90 min; ^{1}H NMR ($CDCl_3$): δ = 0.84 (d, *J* = 6.6 Hz, 3H; ValMe), 0.87 (d, *J* = 6.8 Hz, 3H; ValMe), 1.17 (d, *J* = 6.8 Hz, 3H; AlaMe), 2.10 (m, 1H; ValHβ), 2.41 (s, 3H; TsMe), 3.13 (d, *J* = 7.6 Hz, 2H; PheHβ), 3.41 (ddd, *J* = 5.6, 6.4, 14.0 Hz, 1H; *iso*SerHβ), 3.49 (ddd, *J* = 6.0, 8.0, 14.0 Hz, 1H; *iso*SerHβ), 3.69 (s, 3H; OMe), 3.79 (dq, *J* = 6.8, 7.6 Hz, 1H; AlaHα), 4.13 (ddd, *J* = 4.6, 6.0, 6.4 Hz, 1H; *iso*SerHα), 4.44 (dd, *J* = 5.2, 8.4 Hz, 1H; ValHα), 4.70 (dt, *J* = 7.6, 8.0 Hz, 1H; PheHα), 5.04 (d, *J* = 4.6 Hz, 1H; *iso*SerOH), 6.14 (d, *J* = 7.6 Hz, 1H; AlaNH), 6.92 (d, *J* = 8.4 Hz, 1H; ValNH), 7.18–7.30 (m, 7H; PheArH and $TsArH_{3,5}$), 7.51 (dd, *J* = 5.6, 8.0 Hz, 1H; *iso*SerNH), 7.52 (d, *J* = 8.0 Hz, 1H; PheNH), 7.73 ppm (m, 2H; $TsArH_{2,6}$); MS (ESI): *m/z* calcd 591.4 $[M+H]^+$ found: 591.3.

Ts-(*S*)-Ala-(*R*)-*iso*Ser-(*S*)-Phe-(*S*)-ValOMe (2 e): 92% pure by RP-HPLC (General Methods); R_t = 4.78 min; ^{1}H NMR ($CDCl_3$): δ = 0.93 (d, *J* = 6.8 Hz, 3H; ValMe), 0.95 (d, *J* = 7.2 Hz, 3H; ValMe), 1.15 (d, *J* = 7.2 Hz, 3H; AlaMe), 2.15 (m, 1H; ValHβ), 2.45 (s, 3H; TsMe), 3.00 (dd, *J* = 7.4, 13.9 Hz, 1H; PheHβ), 3.08 (dd, *J* = 6.9, 13.9 Hz, 1H; PheHβ), 3.43 (ddd, *J* = 3.0, 5.2, 14.2 Hz, 1H; *iso*SerHβ), 3.74 (s, 3H; OMe), 3.87–3.95 (m, 2H; AlaHα and *iso*SerHβ), 4.20 (dd, *J* = 3.0, 6.2 Hz, 1H; *iso*SerHα), 4.51 (dd, *J* = 5.8, 8.1 Hz, 1H; ValHα), 4.55 (ddd, *J* = 6.9, 7.4, 8.0 Hz, 1H; PheHα), 6.39 (d, *J* = 8.1 Hz, 1H; ValNH), 7.19–7.34 (m, 10H; PheArH + $TsArH_{3,5}$ + AlaNH + PheNH + *iso*SerNH), 7.77 ppm (m, 2H; $TsArH_{2,6}$); MS (ESI): *m/z* calcd 591.4 $[M+H]^+$ found: 590.3.

Boc-(*S*)-Ala-(*S*)-*iso*Ser-(*S*)-Phe-(*S*)-ValOMe (2 f): 87% pure by RP-HPLC (General Methods); R_t = 4.86 min; ^{1}H NMR ($CDCl_3$): δ (two conformers in 6:4 ratio) = 0.80 (d, *J* = 7.2 Hz, 3H; ValMe), 0.83 (d, *J* = 6.8 Hz, 3H; ValMe), 1.21* and 1.26 (d, *J* = 6.8 Hz, 3H; AlaMe), 1.37 (s, 9H; *t*Bu), 2.05 (m, 1H; ValHβ), 3.01–3.11 (m, 2H; PheHβ), 3.35 (m, 1H; *iso*SerHβ), 3.48 (m, 1H; *iso*SerHβ), 3.65 (s, 3H; OMe), 4.03–4.08 (m, 2H; AlaHα and *iso*SerHα), 4.38 (m, 1H; ValHα), 4.63 (br. q, 1H; PheHα), 5.05 and 5.31* (br. d, 1H; AlaNH), 6.84 (br. d, 1H; ValNH), 7.19–7.23 (m, 6H; PhArH and *iso*SerNH), 7.55 ppm (br. d, *J* = 8.4 Hz, 1H; PheNH) (* major conformation); MS (ESI): *m/z* calcd 536.7 $[M+H]^+$ found: 536.6.

Solid-phase synthesis of Ac-(*S*)-Ala-(*S*/*R*)-Amo-(*S*)-Phe-Wang (2 h)

Wang resin preloaded with Fmoc-PheOH (0.5 g, 0.4–0.8 mmol g^{-1}, resin particle size: 100–200 mesh) was introduced into a reactor for SPPS. Fmoc was removed with DMF/piperidine (4:1, 5 mL) under MW irradiation for 1 min under mechanical shaking (40 W, monitoring the internal temperature at 45 °C with a built-in ATC-FO advanced fiber optic automatic temperature control). The suspension was filtered, the resin was washed with CH_2Cl_2 (5 mL) and treated with a second portion of DMF/piperidine as described above. The suspension was then filtered, and the resin was washed three times in sequence with CH_2Cl_2 (5 mL) and MeOH (5 mL).

All coupling steps were performed according to the following General Procedure. The resin was swollen in CH_2Cl_2 (5 mL), and a solution of the Fmoc-*N*-protected amino acid (0.6 mmol) and HOBt (0.6 mmol) in DMF (4 mL) was added at r.t. and under a nitrogen atmosphere, followed by HBTU (0.6 mmol) and DIPEA (1.2 mmol). The mixture was mechanically shaken under MW irradiation as described above and, after 10 min, the resin was filtered and washed three times with the sequence CH_2Cl_2 (5 mL) and MeOH (5 mL). Coupling efficacy was determined by means of the Kaiser test. All subsequent deprotection steps were performed as reported above.

Ts-Ala-*iso*Ser-SarNH$_2$ (2 i): Boc-*iso*SerOH and H-SarNH$_2$ were coupled in the same quantities and by the same procedure utilized for the preparation of **1 a** (MW-assisted peptide synthesis). The crude Boc-*iso*Ser-SarNH$_2$ was recovered as described for **1 b**,**c** (85%, 78% pure by analytical RP-HPLC, General methods, R_t = 3.17 min). The dipeptide was N-deprotected according to the General Procedure

for Boc Deprotection, and the corresponding peptide-TFA salt was coupled with Ts-AlaOH under the conditions described above. Compound **2i** was isolated (70%, 92% pure by analytical RP-HPLC, see General Methods, $R_t = 3.54$ min) by flash chromatography over silica gel (EtOAc/MeOH, 95:5). ^{1}H NMR ($CDCl_3$): δ (major conformer) = 1.11 (d, $J = 7.2$ Hz, 3H; AlaMe), 2.37 (s, 3H; TsMe), 3.45 (s, 3H; SarMe), 3.64–3.76 (m, 2H; *iso*SerHβ and AlaHα), 3.82 ($J = 4.4$, 6.2, 13.8 Hz, 1H; *iso*SerHβ), 4.14 (d, $J = 18.2$ Hz, 1H; SarHα), 4.20 (d, $J = 18.2$ Hz, 1H; SarHα), 4.90 (br. t, 1H; *iso*SerHα), 6.31 (d, $J = 6.8$ Hz, 1H; AlaNH), 6.90 (s, 1H; CONH_2), 7.20 (s, 1H; CONH_2), 7.35 (m, 2H; $TsArH_{3,5}$), 7.53 (dd, $J = 5.0$, 6.2 Hz, 1H; *iso*SerNH), 7.66 ppm (m, 2H; $TsArH_{2,6}$); MS (ESI): *m/z* calcd 401.1 $[M+H]^+$ found: 401.2.

Solution-phase synthesis of Amo-peptides 3a–g, 10a, and 10b

DSC (0.36 mmol) was added to a stirred solution of **1** (0.33 mmol) in CH_2Cl_2/DMF (3:1, 4 mL) followed by DIPEA (0.07 mmol) at r.t. and under a nitrogen atmosphere. After 1 h, the solvent was removed under reduced pressure, the residue was diluted with 0.1 M HCl (5 mL), and the mixture was extracted with CH_2Cl_2 (3×5 mL). The combined organic layers were dried over Na_2SO_4, the solvent was evaporated under reduced pressure, and the residue was purified by semipreparative RP-HPLC (General Methods).

Ts-(*S*)-Ala-(*S*)-Amo-(*S*)-PheNH$_2$ (3a): 95% pure by RP-HPLC (General Methods); $R_t = 6.41$ min; ^{1}H NMR ($CDCl_3$): $\delta = 1.17$ (d, $J = 6.8$ Hz, 3H; AlaMe), 2.42 (s, 3H; TsMe), 3.48–3.58 (m, 3H; PheHβ and AmoHβ), 3.69 (ddd, $J = 4.0$, 6.4, 13.8 Hz, 1H; AmoHβ), 3.78 (dq, $J = 6.4$, 6.8 Hz, 1H; AlaHα), 4.73 (dd, $J = 4.0$, 7.6 Hz, 1H; AmoHα), 4.93 (t, $J = 8.4$ Hz, 1H; PheHα), 6.10 (br. d, $J = 6.4$ Hz, 1H; AlaNH), 6.24 (s, 1H; CONH_2), 6.52 (s, 1H; CONH_2), 7.09 (br. t, 1H; AmoNH), 7.19 (m, 2H; $TsArH_{3,5}$), 7.20–7.34 (m, 5H; PhArH), 7.72 ppm (m, 2H; $TsArH_{2,6}$); ^{13}C NMR ($CDCl_3$): $\delta = 18.4$, 21.5, 33.8, 38.9, 52.7, 56.8, 76.7, 127.2, 127.5, 128.9, 129.5, 129.9, 135.8, 136.3, 144.0, 154.7, 170.1, 171.6, 172.9 ppm; MS (ESI): *m/z* calcd 503.2 $[M+H]^+$ found: 503.3; elemental analysis calcd (%) for $C_{23}H_{26}N_4O_7S$: C 54.97, H 5.21, N 11.15, S 6.38; found: C 54.14, H 5.28, N 11.28, S 6.51.

Ts-(*S*)-Ala-(*R*)-Amo-(*S*)-PheNH$_2$ (3b): 96% pure by RP-HPLC (General Methods); $R_t = 6.32$ min; ^{1}H NMR ($CDCl_3$): $\delta = 1.15$ (d, $J = 7.1$ Hz, 3H; AlaMe), 2.43 (s, 3H; TsMe), 3.37 (ddd, $J = 4.4$, 4.8, 14.6 Hz, 1H; AmoHβ), 3.52 (d, $J = 8.7$ Hz, 2H; PheHβ), 3.80 (dq, $J = 7.1$, 8.2 Hz, 1H; AlaHα), 4.12 (ddd, $J = 4.2$, 7.6, 14.6 Hz, 1H; AmoHβ), 4.70 (dd, $J = 4.2$, 4.4 Hz, 1H; AmoHα), 4.97 (t, $J = 8.7$ Hz, 1H; PheHα), 6.28 (m, 2H; CONH_2 and AlaNH), 6.41 (s, 1H; CONH_2), 6.99 (dd, $J = 4.8$, 7.6 Hz, 1H; AmoNH), 7.23–7.31 (m, 5H; PheArH), 7.33 (m, 2H; $TsArH_{3,5}$), 7.73 ppm (m, 2H; $TsArH_{2,6}$); ^{13}C NMR ($CDCl_3$): $\delta = 18.7$, 21.3, 33.2, 38.5, 52.5, 55.8, 76.7, 126.8, 127.0, 128.5, 128.6, 129.5, 136.1, 137.0, 143.3, 153.9, 169.3, 170.8, 172.6 ppm; MS (ESI): *m/z* calcd 503.2 $[M+H]^+$ found: 503.3; elemental analysis calcd (%) for $C_{23}H_{26}N_4O_7S$: C 54.97, H 5.21, N 11.15, S 6.38; found: C 56.07, H 5.11, N 10.93, S 6.27.

Ts-(*S*)-Ala-(*S*)-Amo-(*R*)-PheNH$_2$ (3c): 95% pure by RP-HPLC (General Methods); $R_t = 6.88$ min; ^{1}H NMR ($CDCl_3$): $\delta = 1.11$ (d, $J = 7.2$ Hz, 3H; AlaMe), 2.42 (s, 3H; TsMe), 3.45–3.52 (m, 3H; AmoHβ and PheHβ), 3.75–3.84 (m, 2H; AlaHα and AmoHβ), 4.69 (dd, $J = 4.0$, 4.4 Hz, 1H; AmoHα), 4.91 (dd, $J = 6.4$, 9.9 Hz, 1H; PheHα), 6.25 (d, $J = 7.2$ Hz, 1H; AlaNH), 6.47 (s, 1H; CONH_2), 6.79 (s, 1H; CONH_2), 7.18–7.31 (m, 8H; $TsArH_{3,5}$ and PheArH and AmoNH), 7.73 ppm (m, 2H; $TsArH_{2,6}$); ^{13}C NMR ($CDCl_3$): $\delta = 18.3$, 21.0, 33.0, 38.5, 52.2, 55.6, 76.6, 126.6, 126.7, 128.3, 128.4, 129.3, 136.0, 136.8, 143.0, 153.8, 169.1, 170.3, 172.4 ppm; MS (ESI) *m/z* calcd 503.2 $[M+H]^+$ found: 503.3; elemental analysis calcd (%) for $C_{23}H_{26}N_4O_7S$: C 54.97, H 5.21, N 11.15, S 6.38; found: C 55.62, H 5.16, N 11.24, S 6.20.

Ts-(*S*)-Ala-(*S*)-Amo-(*S*)-Phe-(*S*)-ValOMe (3d): 96% pure by RP-HPLC (General Methods); $R_t = 6.55$ min; ^{1}H NMR ($CDCl_3$): $\delta = 0.81$ (d, $J = 6.4$ Hz, 3H; ValMe), 0.88 (d, $J = 6.8$ Hz, 3H; ValMe), 1.13 (d, $J = 7.2$ Hz, 3H; AlaMe), 2.14 (m, 1H; ValHβ), 2.39 (s, 3H; TsMe), 3.44 (ddd, $J = 3.5$, 5.2, 14.4 Hz, 1H; AmoHβ), 3.53 (d, $J = 8.6$ Hz, 2H; PheHβ), 3.63 (ddd, $J = 4.0$, 6.0, 14.4 Hz, 1H; AmoHβ), 3.73 (s, 3H; OMe), 3.82 (dq, $J = 7.2$, 8.6 Hz, 1H; AlaHα), 4.51 (dd, $J = 4.8$, 8.6 Hz, 1H; ValHα), 4.67 (dd, $J = 3.5$, 4.0 Hz, 1H; AmoHα), 4.95 (t, $J = 8.6$ Hz, 1H; PheHα), 5.79 (d, $J = 8.6$ Hz, 1H; AlaNH), 6.81 (d, $J = 8.6$ Hz, 1H; ValNH), 7.00 (dd, $J = 5.2$, 6.0 Hz, 1H; AmoNH), 7.23–7.33 (m, 7H; $PheArH_2$ and $TsArH_{3,5}$), 7.68 ppm (m, 2H; $TsArH_{2,6}$); ^{13}C NMR ($CDCl_3$): $\delta = 17.8$, 18.8, 18.9, 21.4, 30.9, 34.1, 38.9, 52.3, 52.4, 57.4, 57.9, 77.3, 127.0, 127.4, 128.8, 128.9, 129.6, 135.7, 136.9, 143.5, 154.4, 167.5, 171.1, 172.2, 172.5 ppm; MS (ESI): *m/z* calcd 617.2 $[M+H]^+$ found: 617.5; elemental analysis calcd (%) for $C_{29}H_{36}N_4O_9S$: C 56.48, H 5.88, N 9.09, S 5.20; found: C 55.35, H 5.76, N 9.27, S 5.32.

Ts-(*S*)-Ala-(*R*)-Amo-(*S*)-Phe-(*S*)-ValOMe (3e): 94% pure by RP-HPLC (General Methods); $R_t = 6.98$ min; ^{1}H NMR ($CDCl_3$): $\delta = 0.81$ (d, $J = 6.8$ Hz, 3H; ValMe), 0.89 (d, $J = 6.4$ Hz, 3H; ValMe), 1.14 (d, $J = 7.0$ Hz, 3H; AlaMe), 2.14 (m, 1H; ValHβ), 2.44 (s, 3H; TsMe), 3.28 (ddd, $J = 3.0$ 3.4, 14.4 Hz, 1H; AmoHβ), 3.54 (dd, $J = 8.0$, 14.6 Hz, 1H; PheHβ), 3.58 (dd, $J = 8.4$, 14.6 Hz, 1H; PheHβ), 3.77 (s, 3H; OMe), 3.87 (dq, $J = 7.0$, 8.8 Hz, 1H; AlaHα), 4.28 (ddd, $J = 4.1$, 9.0, 14.4 Hz, 1H; AmoHβ), 4.49 (dd, $J = 5.0$, 8.2 Hz, 1H; ValHα), 4.76 (dd, $J = 3.0$, 4.1 Hz, 1H; AmoHα), 5.03 (dd, $J = 8.0$, 8.4 Hz, 1H; PheHα), 6.21 (d, $J = 8.8$ Hz, 1H; AlaNH), 6.41 (d, $J = 8.2$ Hz, 1H; ValNH), 6.78 (dd, $J = 3.4$, 9.0 Hz, 1H; AmoNH), 7.30–7.34 (m, 5H; PheArH), 7.38 (m, 2H, $TsArH_{3,5}$), 7.72 ppm (m, 2H; $TsArH_{2,6}$); ^{13}C NMR ($CDCl_3$): $\delta = 17.8$, 18.7, 18.9, 21.5, 30.9, 34.0, 38.3, 52.4, 52.9, 55.5, 58.3, 77.8, 127.0, 127.1, 127.9, 128.8, 128.9, 129.2, 129.4, 129.8, 129.9, 135.3, 137.1, 143.7, 153.9, 167.4, 171.2, 171.5, 172.5 ppm; MS (ESI): *m/z* calcd 617.2 $[M+H]^+$ found: 617.5; elemental analysis calcd (%) for $C_{29}H_{36}N_4O_9S$: C 56.48, H 5.88, N 9.09, S 5.20; found: C 55.57, H 5.97, N 8.90, S 5.04.

Boc-(*S*)-Ala-(*S*)-Amo-(*S*)-Phe-(*S*)-ValOMe (3f): 95% pure by RP-HPLC (General Methods); $R_t = 7.02$ min; ^{1}H NMR ($CDCl_3$): $\delta = 0.84$ (d, $J = 6.4$ Hz, 3H; ValMe), 0.92 (d, $J = 6.8$ Hz, 3H; ValMe), 1.25 (d, $J = 6.0$ Hz, 3H; AlaMe), 1.42 (s, 9H; *t*Bu), 2.18 (m, 1H; ValHβ), 3.42 (ddd, $J = 4.4$, 5.6, 14.4 Hz, 1H; AmoHβ), 3.53 (d, $J = 8.5$ Hz, 2H; PheHβ), 3.76 (s, 3H; OMe), 3.84 (ddd, $J = 4.8$, 7.2, 14.4 Hz, 1H; AmoHβ), 4.16 (m, 1H; AlaHα), 4.56 (dd, $J = 4.8$, 8.2 Hz, 1H; ValHα), 4.74 (dd, $J = 4.4$, 4.8 Hz, 1H; AmoHα), 4.95 (t, $J = 8.5$ Hz, 1H; PheHα), 5.30 (br. d, 1H; AlaNH), 6.81 (d, $J = 8.2$ Hz, 1H; ValNH), 6.87 (dd, $J = 5.6$, 7.2 Hz, 1.H; AmoNH), 7.23–7.34 ppm (m, 5H; PheArH); ^{13}C NMR ($CDCl_3$): $\delta = 17.6$, 18.5, 18.9, 25.4, 25.5, 28.2, 30.9, 34.2, 38.8, 50.0, 52.4, 57.3, 57.7, 76.6, 127.5, 128.6, 128.8, 129.0, 135.5, 152.1, 154.4, 168.7, 171.4, 172.3, 173.9 ppm; MS (ESI): *m/z* calcd 585.3 $[M+Na]^+$ found: 585.3; elemental analysis calcd (%) for $C_{27}H_{38}N_4O_9$: C 57.64, H 6.81, N 9.96; found: C 56.66, H 6.95, N 10.11.

Boc-(*S*)-Amo-(*S*)-PheNH$_2$ (3g): 96% pure by RP-HPLC (General Methods); $R_t = 6.88$ min; ^{1}H NMR ($CDCl_3$): $\delta = 1.42$ (s, 9H; *t*Bu), 3.23 (ddd $J = 4.4$, 5.4, 14.6 Hz, 1H; AmoHβ), 3.43 (ddd, $J = 4.0$, 7.8, 14.6 Hz, 1H; AmoHβ), 3.46–3.53 (m, 2H; PheHβ), 4.70 (dd, $J = 4.0$, 4.8 Hz, 1H; AmoHα), 4.85–4.94 (m, 2H; AmoNH and PheHα), 5.84 (br. s, 1H; $CONH_2$), 6.43 (br. s, 1H; $CONH_2$), 7.20 (d, $J = 6.8$ Hz, 2H; PheArH), 7.26–7.35 ppm (m, 3H; PheArH); ^{13}C NMR ($CDCl_3$): $\delta = 28.2$, 33.5, 38.5, 56.0, 79.8, 80.9, 127.1, 128.7, 128.4, 136.5, 154.3, 155.7, 169.4, 171.1 ppm; MS (ESI): *m/z* calcd 400.2 $[M+Na]^+$ found: 400.4; elemental analysis calcd (%) for $C_{18}H_{23}N_3O_6$: C 57.29, H 6.14, N 11.13; found: C 58.43, H 6.26, N 10.91.

Solid-phase synthesis of Ac-(*S*)-Ala-(*S*/*R*)-Amo-(*S*)-PheOH (3 h)

The resin-bound peptide **2 h** was suspended in CH_2Cl_2/DMF (3:1, 4 mL), and DSC (0.9 mmol) and DIPEA (0.3 mmol) were added at r.t. and under a nitrogen atmosphere. The reaction was conducted under mechanical shaking for 2 h, then the suspension was filtered and the resin was washed three times in sequence with CH_2Cl_2 (5 mL) and MeOH (5 mL).

The resin-bound peptide was suspended in a solution of TFA (4.8 mL), H_2O (0.20 mL), and phenol (0.050 g), in CH_2Cl_2 (5 mL), and mechanically shaken at r.t. After 2 h, the mixture was filtered, the resin was washed with 10% TFA in Et_2O (2×5 mL) and Et_2O (2× 5 mL). The filtrate and washes were collected and solvent and volatiles were removed at r.t. under N_2 flow. The resulting residue was suspended in ice-cold Et_2O, and the crude solid that precipitated was triturated and collected by centrifuge. Amo-peptide acid **3 h** was isolated as a 1:1 mixture of diastereoisomers by semipreparative RP-HPLC (see General Methods) (80% based on the average resin loading of 0.6 mmol g^{-1}; >95% pure by analytical RP-HPLC). ^{1}H NMR ([D$_6$]DMSO): δ = 1.14 and 1.16 (d, J = 8.0 Hz, 6H; AlaMe), 1.81 (s, 6H; Ac), 2.83 (ddd, J = 3.2, 4.0, 14.2 Hz, 1H; AmoHβ), 3.17–3.29 (m, 3H; AmoHβ and PheHβ), 3.38–3.48 (m, 3H; AmoHβ and PheHβ), 3.49 (ddd, J = 3.6, 8.6, 14.4 Hz, 1H; AmoHβ), 4.17–4.26 (m, 2H; AlaHα), 4.82–4.94 (m, 2H; PheHα), 4.97 (dd, J = 3.6, 7.2 Hz, 1H; AmoHα), 5.10 (dd, 3.2, 7.6 Hz, 1H; AmoHα), 7.18–7.30 (m, 10H; PhArH), 7.90 (br. d, 1H; AlaNH), 7.92–8.04 (m, 2H; AlaNH and AmoNH), 8.19 ppm (br. t, 1H; AmoNH); ^{13}C NMR ([D$_6$]DMSO): δ = 18.1, 18.2, 33.0, 33.1, 48.0, 48.1, 54.2, 54.5, 77.8, 78.1, 126.9, 128.1, 128.5, 128.8, 128.9, 129.1, 136.6, 136.7, 154.0, 168.9, 169.0, 170.3, 170.4, 172.1, 172.7. 173.0, 173.1 ppm; MS (ESI): *m*/*z* calcd $[M+H]^+$ 392.2; found: 392.2; elemental analysis calcd (%) for $C_{18}H_{21}N_3O_7$: C 55.24, H 5.41, N 10.74; found: C 54.14, H 5.52, N 10.55.

Ts-Ala-Oxd-SarNH$_2$ (4): A solution of peptide **2 i** (0.1 g, 0.25 mmol) in CH_2Cl_2/DMF (3:1, 4 mL) was treated with DSC (0.20 g, 0.75 mmol) and DBU (38 μL, 0.25 mmol) at 40 °C and under a nitrogen atmosphere. After 6 h, the reaction was stopped and workup was performed as described for the synthesis of **3 a**–**g**. The Oxd-peptide **4** was isolated by semipreparative RP-HPLC (58 mg, 55%, 94% pure by RP-HPLC; General Methods; R_f = 4.60 min). ^{1}H NMR ($CDCl_3$): δ (major conformer) = 1.32 (d, J = 7.3 Hz, 3H; AlaMe), 2.40 (s, 3H; Ts*Me*), 3.47 (s, 3H; SarMe), 3.90 (dd, J = 4.2, 8.6 Hz, 1H; OxdH$_4$), 4.09 (d, J = 18.0 Hz, 1H; SarHα), 4.12 (dd, J = 8.6, 9.3 Hz, 1H; OxdH$_4$), 4.24 (d, J = 18.0 Hz, 1H; SarHα), 5.11 (dq, J = 7.3, 8.8 Hz, 1H; AlaHα), 5.45 (dd, J = 4.2, 9.3 Hz, 1H; OxdH$_5$), 6.07 (br. s, 1H; CONH$_2$), 6.38 (br. s, 1H; CONH$_2$), 6.44 (m, 2H; CONH$_2$ and AlaNH), 7.18 (m, 2H; TsArH$_{3,5}$), 7.75 ppm (m, 2H; TsArH$_{2,6}$); ^{13}C NMR ([D$_6$]DMSO): δ = 18.5, 20.8, 39.1, 38.6, 50.7, 60.5, 85.4, 128.3, 129.3, 137.6, 141.5, 153.1, 168.4, 169.1, 175.0 ppm; MS (ESI): *m*/*z* calcd $[M+H]^+$ 427.1; found: 427.1; elemental analysis calcd (%) for $C_{17}H_{22}N_4O_7S$: C 47.88, H 5.20, N 13.14; found: C 47.11, H 5.12, N 13.29.

Ts-(*S*)-Ala-(4*R*,5*R*)-4-hydroxy-5-aminomethylOxd-(*S*)-PheNH$_2$ (5): $NaBH_4$ (4 mmol) was added to a solution of **3 b** (0.4 mmol) in MeOH (4 mL) at 0 °C under a nitrogen atmosphere. The mixture was stirred for 7 h, then the reaction was stopped with acetone (4 mL). The reaction mixture was concentrated under reduced pressure and the residue was diluted with water (5 mL), and extracted with CH_2Cl_2 (3×5 mL). The collected organic layers were dried with Na_2SO_4, filtered, and concentrated under reduced pressure. The residue was purified by semipreparative RP-HPLC (see General Methods) to give **5** (85%, 95% pure by RP-HPLC, general Methods, R_f = 5.12 min). ^{1}H NMR ($CDCl_3$): δ = 1.17 (d, J = 6.8 Hz, 3H; AlaMe), 2.44 (s, 3H; TsMe), 3.04 (ddd, J = 3.4, 5.0, 14.6 Hz; C*H*$_2$N), 3.14–3.25 (m, 2H; C*H*$_2$N and PheHβ) 3.34 (dd, J = 7.6, 14.0 Hz, 1H; PheHβ), 3.73 (dq, J = 6.8, 7.2 Hz, 1H; AlaHα), 4.35 (br. t, 1H; OxdH5), 4.84 (dd, J = 7.6, 8.6 Hz, 1H; PheHα), 5.21 (br. s, 1H; OxdH4), 5.95 (br. s, 1H; CON*H*$_2$), 6.03 (d, J = 7.2 Hz, 1H; AlaNH), 6.63 (br. s, 1H;; CON*H*$_2$), 7.08 (dd, J = 5.0, 6.8 Hz, 1H; CH$_2$N*H*), 7.27–7.35 (m, 7H; PhArH and TsArH$_{3,5}$), 7.73 ppm (m, 2H; TsArH$_{2,6}$); ^{13}C NMR ($CDCl_3$): δ = 19.2, 20.8, 34.8, 40.1, 52.7, 60.2, 79.7, 81.6, 125.7, 127.0, 127.6, 128.8, 129.0, 129.3, 130.1, 135.5, 138.1, 144.2, 157.3, 171.2, 172.9 ppm elemental analysis calcd (%) for $C_{23}H_{28}N_4O_7S$: C 54.75, H 5.59, N 11.10, S 6.36; found: C 53.98, H 5.64, N 11.32, S 6.55; MS (ESI): *m*/*z* calcd $[M+Na]^+$ 527.2; found: 527.0.

Ts-(*S*)-Ala-(*S*)-α-Me-*iso*SerOMe (8 a): Nitromethane (1.5 mL), methyl pyruvate (50 μL, 0.5 mmol), and TEA (14 μL, 0.1 mmol) were mixed in the presence of Cu(OTf)$_2$ (36 mg, 0.10 mmol) and 2,2′-isopropylidenebis[(4*R*)-4-*tert*-butyl-2-oxazoline] (31 mg, 0.10 mmol), as described previously (Ref.[30] main text). The reaction mixture was filtered through a plug of silica, and solvent was removed under reduced pressure. The resulting crude α-nitro-(*S*)-hydroxy ester **6 a**, which was obtained in quantitative yield, was identified by RP-HPLC-ESI analysis, and utilized without further purification (81 mg, 99%, 85% pure by RP-HPLC analysis; R_t = 2.04 min; 87% *ee* as determined by chiral HPLC analysis of the crude mixture, see General Methods). MS (ESI): *m*/*z* calcd $[M+Na]^+$ 186.1; found: 186.2. Compound **6 a** was dissolved in EtOH (6 mL) and treated with 10% Pd/C (100 mg) and H_2 at atmospheric pressure for 6 h at r.t. to give, after filtration over Celite and evaporation of solvent under reduced pressure, 3-amino-2-hydroxy-2-methyl-propionic ester **7 a** (67 mg, 99%, 82% pure by RP-HPLC analysis, see General Methods; R_t = 1.67 min), which was utilized for the next step without purification. MS (ESI): *m*/*z* calcd $[M+H]^+$ 134.1; found: 134.1. Crude **7 a** was coupled with Ts-AlaOH (120 mg, 0.5 mmol) by using the same procedure described for the synthesis of **1 a**. After the usual workup, dipeptide **8 a** (140 mg, 80%, 88% pure by RP-HPLC analysis, see General Methods; R_t = 3.85 min) was isolated by flash chromatography over silica gel (EtOAc/cyclohexane, 2:8). ^{1}H NMR ($CDCl_3$): δ = 1.25 (d, J = 6.7 Hz, 3H; AlaMe), 1.40 (s, 3H; *Me-iso*Ser), 2.44 (s, 3H; TsMe), 3.32 (dd, J = 6.0, 14.0 Hz; *iso*SerHβ), 3.66–3.83 (m, 5H; AlaHα and Me-*iso*SerHβ and COOMe), 4.95 (br. d, J = 8.4 Hz, 1H; AlaNH), 6.47 (dd, J = 5.0, 6.0 Hz, 1H; *iso*SerNH),7.33 (m, 2H; TsArH$_{3,5}$), 7.75 ppm (m, 2H; TsArH$_{2,6}$); MS (ESI): *m*/*z* calcd $[M+H]^+$ 359.1; found: 359.3.

Ts-(*S*)-Ala-(*R*)-α-Me-*iso*SerOMe (8 b): The reaction of nitromethane and methyl pyruvate in the same quantities as described for the preparation of **6 a** in the presence of 2,2′-isopropylidenebis[(4*S*)-4-*tert*-butyl-2-oxazoline], gave **6 b** in quantitative yield (87% pure by RP-HPLC analysis; R_t = 2.04 min; 89% *ee* as determined by chiral HPLC analysis of the crude mixture, see General Methods). MS (ESI): *m*/*z* calcd $[M+Na]^+$ 186.1; found: 186.1. The reduction to β-amino ester **7 b** and coupling with Ts-AlaOH gave **8 b**, after purification by flash chromatography (150 mg, 84%; 93% pure by RP-HPLC analysis, see General Methods; R_t = 3.85 min) was done as described for **8 a**. ^{1}H NMR ($CDCl_3$): δ = 1.23 (d, J = 6.7 Hz, 3H; AlaMe), 1.37 (s, 3H; *Me-iso*Ser), 2.44 (s, 3H; TsMe), 3.20 (dd, J = 4.8, 13.6 Hz, 1H; *iso*SerHβ), 3.66–3.83 (m, 5H; AlaHα and *iso*SerHβ and COOMe), 5.06 (br. d, J = 8.0 Hz, 1H; AlaNH), 6.65 (br. t, 1H; *iso*SerNH), 7.33 (m, 2H; TsArH$_{3,5}$), 7.75 (m, 2H; TsArH$_{2,6}$); MS (ESI): *m*/*z* calcd $[M+H]^+$ 359.1; found: 359.3.

Ts-(*S*)-Ala-(*S*)-α-Me-*iso*Ser-(*S*)-Phe-(*S*)-ValOMe (9 a): Dipeptide ester **8 a** (140 mg, 0.39 mmol) was dissolved in MeOH (2 mL) and treated with 1 M LiOH (1 mL) while stirring. After 6 h, the pH was adjusted to 7 with 0.1 M HCl and the solvent was removed under reduced pressure to give Ts-Ala-α-Me-*iso*SerOH (128 mg, 95%, 90% pure by RP-HPLC analysis, see General Methods; R_t = 2.35 min). MS (ESI): *m*/

z calcd $[M+H]^+$ 345.1; found: 345.2. The residue was suspended in CH_2Cl_2/DMF (4:1, 5 mL) and treated with HOBt, HBTU, DIPEA, and H-Phe-ValOMe under MW irradiation as described for the preparation of **1a**. After the usual workup, tetrapeptide **9a** (0.20 g, 85%, 90% pure by analytical RP-HPLC, see General Methods; R_f= 4.99 min) was isolated by flash chromatography over silica gel (EtOAc). ^{1}H NMR ($CDCl_3$): δ= 0.79 (d, J=5.8 Hz, 3H; ValMe), 0.82 (d, J=6.8 Hz, 3H; ValMe), 1.09 (d, J=6.8 Hz, 3H; AlaMe), 1.22 (s, 3H; α-*Me-iso*Ser), 2.07 (m, 1H; ValHβ), 2.36 (s, 3H; TsMe), 3.05 (dd, J= 8.0, 14.8 Hz, 1H; PheHβ), 3.10 (dd, J=6.8, 14.8 Hz, 1H; PheHβ), 3.29 (d, J=5.8 Hz, 2H; *iso*SerHβ), 3.63 (s, 3H; OMe), 3.67 (dq, J= 6.8, 7.6 Hz, 1H; AlaHα), 4.38 (dd, J=4.8, 8.0 Hz, 1H; ValHα), 4.48 (ddd, J=6.8, 7.6, 8.0 Hz, 1H; PheHα), 6.69 (d, J=7.6 Hz, 1H; AlaNH), 6.96 (d, J=8.0 Hz, 1H; ValNH), 7.17–7.27 (m, 7H; PheArH and $TsArH_{3,5}$), 7.38 (t, J=5.8 Hz, 1H; *iso*SerNH), 7.50 (d, J=7.6 Hz, 1H; PheNH), 7.66 ppm (m, 2H; $TsArH_{2,6}$); MS (ESI): *m/z* calcd $[M+H]^+$ 605.3; found: 605.5.

Ts-(*S*)-Ala-(*R*)-α-Me-*iso*Ser-(*S*)-Phe-(*S*)-ValOMe (9b): Dipeptide ester **8b** (150 mg, 0.42 mmol) was treated with 1 M LiOH in MeOH as described for **7a**, affording the dipeptide acid (134 mg, 95%, 85% pure by RP-HPLC analysis, see General Methods; R_t= 2.38 min) after the same reaction workup. MS (ESI): *m/z* calcd $[M+H]^+$ 345.1; found: 345.3. Ts-Ala-(*R*)-α-Me-*iso*SerOH was coupled with H-Phe-ValOMe, as described for the preparation of **9a**. Tetrapeptide **9b** (0.21 g, 83%, 91% pure by analytical RP-HPLC, see General Methods; R_f=5.11 min) was isolated after the same work up described for **9a**. ^{1}H NMR ($CDCl_3$): δ= 0.87 (d, J=5.6 Hz, 3H; ValMe), 0.86 (d, J=6.8 Hz, 3H; ValMe), 1.03 (d, J=7.2 Hz, 3H; AlaMe), 1.15 (s, 3H; α-*Me-iso*Ser), 2.06 (m, 1H; ValHβ), 2.35 (s, 3H; TsMe), 2.89 (dd, J=8.0, 14.2 Hz, 1H; PheHβ), 3.05 (dd, J=6.4, 14.2 Hz, 1H; PheHβ), 3.17 (dd, J=5.6, 13.6 Hz, 1H; *iso*SerHβ), 3.51 (dd, J=6.8, 13.6 Hz, 1H; *iso*SerHβ), 3.65 (s, 3H; OMe), 3.76 (dq, J= 7.2, 7.8 Hz, 1H; AlaHα), 4.40 (dd, J=5.8, 8.2 Hz, 1H; ValHα), 4.53 (ddd, J=6.4, 7.6, 8.0 Hz, 1H; PheHα), 6.80 (d, J=7.8 Hz, 1H; AlaNH), 7.09–7.15 (m, 3H; ValNH and $PheArH_{3,5}$), 7.18–7.26 (m, 6H; $PheArH_{2,4,6}$ and $TsArH_{3,5}$ and *iso*SerNH), 7.35 (d, J=7.6 Hz, 1H; PheNH), 7.66 (m, 2H; $TsArH_{2,6}$); MS (ESI): *m/z* calcd $[M+H]^+$ 605.3; found: 605.5.

Ts-(*S*)-Ala-(*S*)-5-Me-Amo-(*S*)-Phe-(*S*)-ValOMe (10a): The cyclization of **9a** in solution as reported for **3a–g** followed by the same workup of the reaction and isolation by semipreparative RP-HPLC, afforded **10a** (95%, 96% pure by analytical RP-HPLC, see General methods; R_t=7.23 min). ^{1}H NMR ($CDCl_3$): δ=0.87 (d, J=7.2 Hz, 3H; ValMe), 0.94 (d, J=7.2 Hz, 3H; ValMe), 1.14 (d, J=6.8 Hz, 3H; AlaMe), 1.31 (s, 3H; AmoMe), 2.22 (m, 1H; ValHβ), 2.42 (s, 3H; TsMe), 3.33 (dd, J=4.8, 14.4 Hz, 1H; AmoHβ), 3.49 (dd, J=7.4, 14.0 Hz, 1H; PheHβ), 3.55 (dd, J=10.4, 14.0 Hz, 1H; PheHβ), 3.67 (dd, J=7.6, 14.4 Hz, 1H; AmoHβ), 3.80 (s, 3H; OMe), 3.88 (dq, J= 6.8, 8.8 Hz, 1H; AlaHα), 4.57 (dd, J=4.6, 8.2 Hz, 1H; ValHα), 4.95 (dd, J=7.4, 10.4 Hz, 1H; PheHα), 5.64 (d, J=8.8 Hz, 1H; AlaNH), 6.76 (d, J=8.2 Hz, 1H; ValNH), 6.97 (dd, J=4.8, 7.6 Hz, 1H; AmoNH), 7.24–7.36 (m, 7H; PheArH and $TsArH_{3,5}$), 7.70 ppm (m, 2H; $TsArH_{2,6}$); ^{13}C NMR ($CDCl_3$): δ= 17.5, 19.0, 19.3, 19.7, 21.5, 31.0, 34.4, 43.5, 52.2, 52.7, 57.8, 58.1, 84.3, 127.0, 127.1, 127.9, 128.8, 128.8, 128.9, 129.1, 129.3, 129.7, 129.9, 135.0, 137.2, 143.5, 153.6, 167.7, 172.2, 172.5, 174.6 ppm; MS (ESI): *m/z* calcd $[M+H]^+$ 631.2; found: 631.1; elemental analysis calcd (%) for $C_{30}H_{38}N_4O_9S$: C 57.13, H 6.07, N 8.88, S 5.08; found: C 58.27, H 6.18, N 8.81, S 4.97.

Ts-(*S*)-Ala-(*R*)-5-Me-Amo-(*S*)-Phe-(*S*)-ValOMe (10b). The cyclization of **9b** in solution as reported for **3a–g** and **9a** followed by the same workup of the reaction and isolation by semipreparative RP-HPLC afforded **10b** (92% 97% pure by analytical RP-HPLC, see General Methods; R_t=7.45 min). ^{1}H NMR ($CDCl_3$): δ=0.87 (d, J= 7.2 Hz, 3H; ValMe), 0.94 (d, J=7.2 Hz, 3H; ValMe), 1.13 (d, J= 7.2 Hz, 3H; AlaMe), 1.23 (s, 3H; AmoMe), 2.19 (m, 1H; ValHβ), 2.44 (s, 3H; TsMe), 3.12 (dd, J=3.6, 14.4 Hz, 1H; AmoHβ), 3.48 (dd, J= 9.6, 14.0 Hz, 1H; PheHβ), 3.54 (dd, J=7.8, 14.0 Hz, 1H; PheHβ), 3.79 (s, 3H; OMe), 3.86 (dq, J=7.2. 8.8 Hz, 1H; AlaHα), 4.09 (dd, J= 9.2, 14.4 Hz, 1H; AmoHβ), 4.51 (dd, J=4.8, 8.2 Hz, 1H; ValHα), 4.99 (dd, J=7.8, 9.6 Hz, 1H; PheHα), 6.34 (d, J=8.8 Hz, 1H; AlaNH), 6.52 (d, J=8.2 Hz, 1H; ValNH), 6.76 (dd, J=3.6, 9.2 Hz, 1H; AmoNH), 7.19–7.32 (m, 5H; PheArH), 7.38 (m, 2H; $TsArH_{3,5}$), 7.72 ppm (m, 2H; $TsArH_{2,6}$); ^{13}C NMR ($CDCl_3$): δ=18.0, 18.4, 18.6, 21.1, 22.1, 31.4, 33.2, 43.0, 51.8, 52.3, 55.4, 58.0, 84.2, 126.4, 126.7, 128.3, 128.6, 129.4, 136.0, 137.0, 142.9, 156.1, 167.6, 171.8, 172.1, 173.5. MS (MS): *m/z* calcd $[M+H]^+$ 631.2; found: 631.1; elemental analysis calcd (%) for $C_{30}H_{38}N_4O_9S$: C 57.13, H 6.07, N 8.88, S 5.08; found: C 56.00, H 5.99, N 8.91, S 5.13.

ROESY and molecular dynamics

2D ROESY experiments in $[D_6]$DMSO/H_2O (8:2) were performed in the phase-sensitive mode at r.t., spin-locking field (γb2) was 2000 Hz, and mixing time was set to 250 ms; spectra were processed in the hypercomplex approach; peaks were calibrated on DMSO. Only ROESY-derived constraints were included in the restrained molecular dynamics.[50] Cross-peak intensities were classified as very strong, strong, medium, and weak, and were associated with distances of 2.3, 2.7, 3.3, and 5.0 Å, respectively.[51] The intensities of the cross peaks arising from protons separated by known distances (e.g., geminal) were found to match with these associations. Geminal and other clear correlations were discarded as constraints. For the absence of Hα(*i*, *i*+1) ROESY cross peaks, all of the ω bonds were set at 180° (force constant: 16 kcal mol^{-1} Å^{-2}).

MD simulations

The restrained MD simulations were conducted at 300 K and 1 atm by using the AMBER force field in a 30×30×30 Å box of standard TIP3P models of equilibrated water.[52] Periodic boundary conditions were applied, a dielectric constant of 1 was used, and the cutoff distance for the nonbonded interactions was 12 Å. All water molecules with atoms that come closer than 2.3 Å to a solute atom were eliminated. A 100 ps simulation at 1200 K was used for generating 50 random structures that were subsequently subjected to a 50 ps restrained MD with a 50% scaled force field at the same temperature, followed by 50 ps with full restraints (distance force constant of 7 kcal mol^{-1} Å^{-2}), after which the system was cooled in 20 ps to 50 K. H-bond interactions were not included, nor were torsion angle restraints. The resulting structures were minimized with 3000 cycles of steepest descent and 3000 cycles of conjugated gradient (convergence of 0.01 kcal Å^{-1} mol^{-1}). The backbones of the structures were clustered by the rmsd analysis.[50]

Unrestrained MD simulations[50] were performed starting with the conformation derived from ROESY in a 30×30×30 Å box of standard TIP3P water for 10 ns at 298 K using periodic boundary conditions, at constant temperature and pressure (Berendsen scheme,[53] bath relaxation constant of 0.2). For 1–4 scale factors, van der Waals and electrostatic interactions are scaled in AMBER to half their nominal value. The integration time step was set to 0.1 fs. The system coordinates were collected every picosecond.

Computational methods

Theoretical calculations and full molecular geometry optimizations in the ground state have been performed in vacuo by using the density functional theory (DFT)[54] methods implemented the Gaus-

sian 09 package of programs.[34] In particular, calculations were carried out by combining the three-parameter hybrid functional (B3) for the exchange part[55] and the Lee–Yang–Parr (LYP)[56] to the 6–311++G(d,p) basis set.

Acknowledgements

We thank Fondazione Umberto Veronesi, Milano/Roma, MIUR (PRIN 2010), the Italian Minister for Foreign Affairs (bilateral Proj. Italy-Mexico 2011–13), the Fondazione per la Ricerca sulla Fibrosi Cistica, Verona (FFC#11/2011), for financial support.

Keywords: chain structures · conformation analysis · Freidinger lactams · peptidomimetics · amino acids

[1] L. Gentilucci, A. Tolomelli, F. Squassabia, *Curr. Med. Chem.* **2006**, *13*, 2449 – 2466.
[2] L. Gentilucci, R. De Marco, L. Cerisoli, *Curr. Pharm. Des.* **2010**, *16*, 3185 – 3203.
[3] a) V. J. Hruby, P. M. Balse, *Curr. Med. Chem.* **2000**, *7*, 945 – 970; b) R. M. J. Liskamp, D. T. S. Rijkers, J. A. W. Kruijtzer, J. Kemmink, *ChemBioChem* **2011**, *12*, 1626 – 1653.
[4] G. R. Gómez, J. D. A. Tyndall, B. Pfeiffer, G. Abbenante, D. P. Fairlie, *Chem. Rev.* **2010**, *110*, PR1 – PR41.
[5] J. S. Richardson, *Adv. Protein Chem.* **1981**, *34*, 167 – 339.
[6] For some reviews, see: a) A. J. Souers, J. A. Ellman, *Tetrahedron* **2001**, *57*, 7431 – 7448; b) M. MacDonald, J. Aubé, *Curr. Org. Chem.* **2001**, *5*, 417 – 438; c) W. A. Loughlin, J. D. A. Tyndall, M. P. Glenn, D. P. Fairlie, *Chem. Rev.* **2004**, *104*, 6085 – 6117; d) R. F. Hirschmann, K. C. Nicolaou, A. R. Angeles, J. S. Chen, A. B. Smith III, *Acc. Chem. Res.* **2009**, *42*, 1511 – 1520; e) L. R. Whitby, D. L. Boger, *Acc. Chem. Res.* **2012**, *45*, 1698 – 1709; for some selected recent examples, see: f) D. Blomberg, M. Hedenstro, P. Kreye, I. Sethson, K. Brickmann, J. Kihlberg, *J. Org. Chem.* **2004**, *69*, 3500 – 3508; g) X. Gu, J. Ying, R. S. Agnes, E. Navratilova, P. Davis, G. Stahl, F. Porreca, H. I. Yamamura, V. J. Hruby, *Org. Lett.* **2004**, *19*, 3285 – 3288; h) U. Rosenström, C. Sköld, G. Lindeberg, M. Botros, F. Nyberg, A. Karlén, A. Hallberg, *J. Med. Chem.* **2006**, *49*, 6133 – 6137; i) L. Lomlim, J. Einsiedel, F. W. Heinemann, K. Meyer, P. Gmeiner, *J. Org. Chem.* **2008**, *73*, 3608 – 3611; j) Y. Angell, D. Chen, F. Brahimi, H. U. Saragovi, K. Burgess, *J. Am. Chem. Soc.* **2008**, *130*, 556 – 565; k) R. Scheffelaar, R. A. K. Nijenhuis, M. Paravidino, M. Lutz, A. L. Spek, A. W. Ehlers, F. J. J. de Kanter, M. B. Groen, R. V. A. Orru, E. Ruijter, *J. Org. Chem.* **2009**, *74*, 660 – 668; l) M. Sañudo, M. G. Valverde, S. Marcaccini, J. J. Delgado, J. Rojo, T. Torroba, *J. Org. Chem.* **2009**, *74*, 2189 – 2192; m) G. Lesma, N. Landoni, T. Pilati, A. Sacchetti, A. Silvani, *J. Org. Chem.* **2009**, *74*, 8098 – 8105; n) J. Y. Lee, I. Im, T. R. Webb, D. McGrath, M. Song, Y. Kim, *Bioorg. Chem.* **2009**, *37*, 90 – 95; o) A. Mieczkowski, W. Koźmiński, J. Jurczak, *Synthesis* **2010**, *2*, 221 – 232; p) A. Pinsker, J. Einsiedel, S. Harterich, R. Waibel, P. Gmeiner, *Org. Lett.* **2011**, *13*, 3502 – 3505.
[7] a) R. M. Freidinger, D. F. Veber, D. S. Perlow, J. R. Brooks, R. Saperstein, *Science* **1980**, *210*, 656 – 658; b) A. Perdih, D. Kikelj, *Curr. Med. Chem.* **2006**, *13*, 1525 – 1556.
[8] a) J. Aube, in *Advance in Amino Acid Mimetics and Peptidomimetics, Vol. 1* (Ed.: A. Abel), JAI Press, Greenwich, **1997**, 193 – 232; b) A. D. Piscopio, J. E. Robinson, *Curr. Opin. Chem. Biol.* **2004**, *8*, 245 – 254.
[9] L. R. Whitby, Y. Ando, V. Setola, P. K. Vogt, B. L. Roth, D. L. Boger, *J. Am. Chem. Soc.* **2011**, *133*, 10184 – 10194.
[10] a) A. Perdih, D. Kikelj, *Curr. Med. Chem.* **2006**, *13*, 1525 – 1556; b) R. M. Freidinger, *J. Org. Chem.* **1985**, *50*, 3631 – 3633; c) W. L. Scott, J. G. Martynow, J. C. Huffman, M. J. O'Donnell, *J. Am. Chem. Soc.* **2007**, *129*, 7077 – 7088.
[11] a) C. Palomo, J. M. Aizpurua, A. Benito, R. Galarza, U. K. Khamrai, J. Vazquez, B. de Pascual-Teresa, P. M. Nieto, A. Linden, *Angew. Chem.* **1999**, *111*, 3241 – 3244; *Angew. Chem. Int. Ed.* **1999**, *38*, 3056 – 3058; b) C. Palomo, J. M. Aizpurua, A. Benito, J. I. Miranda, R. M. Fratila, C. Matute, M. Domercq, F. Gago, S. Martin-Santamaria, A. Linden, *J. Am. Chem. Soc.* **2003**, *125*, 16243 – 16260; c) J. M. Aizpurua, C. Palomo, E. Balentová, A. Jimenez, E. Andreieff, M. Sagartzazu-Aizpurua, J. I. Miranda, A. Linden, *J. Org. Chem.* **2013**, *78*, 224 – 237.
[12] a) L. Gentilucci, A. Tolomelli, R. De Marco, C. Tomasini, S. Feddersen, *Eur. J. Org. Chem.* **2011**, 4925 – 4930; b) R. De Marco, A. Tolomelli, M. Campitiello, P. Rubini, L. Gentilucci, *Org. Biomol. Chem.* **2012**, *10*, 2307 – 2317; c) R. De Marco, A. Greco, S. Rupiani, A. Tolomelli, C. Tomasini, S. Pieraccini, L. Gentilucci, *Org. Biomol. Chem.* **2013**, *11*, 4273 – 4420.
[13] a) A. Polinsky, M. G. Cooney, A. Toy-Palmer, G. Osapay, M. Goodman, *J. Med. Chem.* **1992**, *35*, 4185 – 4194; b) C. Bonauer, T. Walenzyk, B. König, *Synthesis* **2006**, *1*, 1 – 20.
[14] a) Ö. Demir Ordu, I. Doğan, *Chirality* **2010**, *22*, 641 – 654; b) G. Chen, C. Chunling Fu, S. Ma, *Org. Biomol. Chem.* **2011**, *9*, 105 – 110; c) S. Kano, T. Yokomatsu, H. Nemoto, S. Shibuya, *J. Am. Chem. Soc.* **1986**, *108*, 6746 – 6748.
[15] a) G. Lelais, D. Seebach, *Biopolymers* **2004**, *76*, 206 – 243; b) E. Juaristi, V. Soloshonok, Eds.; Wiley-VCH: New York, **2005**; c) G. Cardillo, C. Tomasini, *Chem. Soc. Rev.* **1996**, *25*, 117 – 128.
[16] C. Toniolo, *Int. J. Peptide Protein Res.* **1990**, *35*, 287 – 300.
[17] For a β2-β3-DKP scaffold, see: A. S. M. Ressurreição, A. Bordessa, M. Civera, L. Belvisi, C. Gennari, U. Piarulli, *J. Org. Chem.* **2008**, *73*, 652 – 660.
[18] a) N. J. Ede, J. D. Rae, M. T. W. Hearn, *Tetrahedron Lett.* **1990**, *31*, 6071 – 6074; b) K. Weber, P. Gmeiner, *Synlett* **1998**, 885 – 886; c) D. Michel, R. Waibel, P. Gmeiner, *Heterocycles* **1999**, *51*, 365 – 372; d) T. Lehmann, D. Michel, M. Glänzel, R. Waibel, P. Gmeiner, *Heterocycles* **1999**, *51*, 1389 – 1400; e) K. Weber, U. Ohnmacht, P. Gmeiner, *J. Org. Chem.* **2000**, *65*, 7406 – 7416; f) P. G. Hoffmann, *Synlett* **2002**, *6*, 1014 – 1016.
[19] a) C. M. Goodman, S. Choi, S. Shandler, W. F. DeGrado, *Nat. Chem. Biol.* **2007**, *3*, 252 – 262; b) W. S. Horne, S. H. Gellman, *Acc. Chem. Res.* **2008**, *41*, 1399 – 1408; c) L. K. Pilsl, O. Reiser, *Amino Acids* **2011**, *41*, 709 – 718; d) A. Roy, P. Prabhakaran, P. K. Baruah, G. J. Sanjayan, *Chem. Commun.* **2011**, *47*, 11593 – 11611; e) T. A. Martinek, F. Fülöp, *Chem. Soc. Rev.* **2012**, *41*, 687 – 702.
[20] a) V. Santagada, F. Fiorino, E. Perissutti, B. Severino, V. De Filippis, B. Vivenzio, G. Caliendo, *Tetrahedron Lett.* **2001**, *42*, 5171 – 5173; b) B. Bacsa, K. Horváti, S. Bösze, F. Andreae, C. O. Kappe, *J. Org. Chem.* **2008**, *73*, 7532 – 7542.
[21] T. Fujisawa, S. Odake, Y. Ogawa, J. Yasuda, Y. Morita, T. Morikawa, *Chem. Pharm. Bull.* **2002**, *50*, 239 – 252.
[22] a) B. D. Zlatopolskiy, M. Radzom, A. Zeeck, A. de Meijere, *Eur. J. Org. Chem.* **2006**, 1525 – 1534; b) S. Liu, Y. Yang, X. Liu, F. K. Ferdousi, A. S. Batsanov, A. Whiting, *Eur. J. Org. Chem.* **2013**, 5692.
[23] M. Ousmer, N. A. Braun, C. Bavoux, M. Perrin, M. A. Ciufolini, *J. Am. Chem. Soc.* **2001**, *123*, 7534 – 7538.
[24] A. Isidro-Llobet, M. Alvarez, F. Albericio, *Chem. Rev.* **2009**, *109*, 2455 – 2504.
[25] T. Fukuyama, C. K. Jow, M. Cheung, *Tetrahedron Lett.* **1995**, *36*, 6373 – 6374.
[26] G. Sabitha, B. V. S. Reddy, S. Abraham, J. S. Yadav, *Tetrahedron Lett.* **1999**, *40*, 1569 – 1570.
[27] T. Ankner, G. Hilmersson, *Org. Lett.* **2009**, *11*, 503 – 506.
[28] G. Zappia, E. Gacs-Baitz, G. Delle Monache, D. Misiti, L. Nevola, B. Botta, *Curr. Org. Synth.* **2007**, *4*, 81 – 135.
[29] For some recent examples, see: a) J. E. Semple, T. D. Owens, K. Nguyen, O. E. Levy, *Org. Lett.* **2000**, *2*, 2769 – 2772; b) Y. Aoyagi, R. P. Jain, R. M. Williams, *J. Am. Chem. Soc.* **2001**, *123*, 3472 – 3477; c) F. Fringuelli, F. Pizzo, M. Rucci, L. Vaccaro, *J. Org. Chem.* **2003**, *68*, 7041 – 7045; d) F. Gassa, A. Contini, G. Fontana, S. Pellegrino, M. L. Gelmi, *J. Org. Chem.* **2010**, *75*, 7099 – 7106; e) Y. Jiang, X. Chen, Y. Zheng, Z. Xue, C. Shu, W. Yuan, X. Zhang, *Angew. Chem.* **2011**, *123*, 7442 – 7445; *Angew. Chem. Int. Ed.* **2011**, *50*, 7304 – 7307; f) F. Rodriguez, F. Corzana, A. Avenoza, J. H. Busto, J. M. Peregrina, M. D. M. Zurbano, *Curr. Top. Med. Chem.* **2014**, *14*, 1225 – 1234.
[30] C. Christensen, K. Juhl, R. G. Hazell, K. A. Jørgensen, *J. Org. Chem.* **2002**, *67*, 4875 – 4881.
[31] a) S. U. Pandya, R. S. Dickins, D. Parker, *Org. Biomol. Chem.* **2007**, *5*, 3842 – 3846; b) K. P. Jayakanthan, M. Y. D. Vankar, *Tetrahedron* **2004**, *60*, 397 – 403.
[32] a) J. Duan, B. W. King, C. Decicco, T. P. , Jr., Maduskuie, M. E. Voss, PCT Int. Appl., WO 2001070734 A2 20010927, **2001**.
[33] a) A. Banerjee, P. Balaram, *Curr. Sci. India* **1997**, *73*, 1067 – 1077; b) Y.-D. Wu, D.-P. Wang, *J. Am. Chem. Soc.* **1999**, *121*, 9352 – 9362; c) F. Schu-

mann, A. Müller, M. Koksch, G. Müller, N. Sewald, *J. Am. Chem. Soc.* **2000**, *122*, 12009 – 12010; d) R. Günther, H.-J. Hofmann, *Helv. Chim. Acta* **2002**, *85*, 2149 – 2168, and references herein; e) S. Sagan, T. Milcent, R. Ponsinet, O. Convert, O. Tasseau, G. Chassaing, S. Lavielle, O. Lequin, *Eur. J. Biochem.* **2003**, *270*, 939 – 949; f) C. Baldauf, R. Günther, H. Hofmann, *Biopolymers* **2006**, *84*, 408 – 413; g) R. Rai, P. G. Vasudev, K. Ananda, S. Raghothama, N. Shamala, I. L. Karle, P. Balaram, *Chem. Eur. J.* **2007**, *13*, 5917 – 5926; h) E. W. Guthöhrlein, M. Malešević, Z. Majer, N. Sewald, *Biopolymers* **2007**, *88*, 829 – 839; i) K. Basuroy, V. Karuppiah, N. Shamala, P. Balaram, *Helv. Chim. Acta* **2012**, *95*, 2589 – 2603.

[34] M. J. Frisch, G. W. Trucks, H. B. Schlegel, G. E. Scuseria, M. A. Robb, J. R. Cheeseman, G. Scalmani, V. Barone, B. Mennucci, G. A. Petersson, H. Nakatsuji, M. Caricato, X. Li, H. P. Hratchian, Izmaylov, A. F. J. Bloino, G. Zheng, J. L. Sonnenberg, M. Hada, M. Ehara, K. Toyota, R. Fukuda, J. Hasegawa, M. Ishida, T. Nakajima, Y. Honda, O. Kitao, H. Nakai, T. Vreven, J. A., Jr., Montgomery, J. E. Peralta, F. Ogliaro, M. Bearpark, J. J. Heyd, E. Brothers, K. N. Kudin, V. N. Staroverov, R. Kobayashi, J. Normand, K. Raghavachari, A. Rendell, J. C. Burant, S. S. Iyengar, J. Tomasi, M. Cossi, N. Rega, J. M. Millam, M. Klene, J. E. Knox, J. B. Cross, V. Bakken, C. Adamo, J. Jaramillo, R. Gomperts, R. E. Stratmann, O. Yazyev, A. J.; R.; Pomelli, C.; Ochterski, J. W.; Martin, R. L.; Morokuma, K.; Zakrzewski, V. G. Austin, R. Cammi, C. Pomelli, J. W. Ochterski, R. L. Martin, K. Morokuma, V. G. Zakrzewski, G. A. Voth, P. Salvador, J. J. Dannenberg, S. Dapprich, A. D. Daniels, O. Farkas, J. B. Foresman, J. V. Ortiz, J. Cioslowski, D. J. Fox, Gaussian 09, Revision B.01; Gaussian, Inc.: Wallingford, CT, **2009**.

[35] a) P. A. Temussi, D. Picone, G. Saviano, P. Amodeo, A. Motta, T. Tancredi, S. Salvadori, R. Tomatis, *Biopolymers* **1992**, *32*, 367 – 372, and references herein; b) A. Borics, G. Töth, *J. Mol. Graphics Modell.* **2010**, *28*, 495 – 505; c) E. Sikorska, M. J. Slusarz, B. Lammek, *Biopolymers* **2006**, *82*, 603 – 614.

[36] a) K. D. Kopple, M. Ohnishi, A. Go, *Biochemistry* **1969**, *8*, 4087 – 4095; b) I. L. Karle, A. Banerjee, S. Bhattacharya, P. Balaram, *Biopolymers* **1996**, *38*, 515 – 525.

[37] a) J. A. Smith, L. G. Pease, *CRC Crit. Rev. Biochem.* **1980**, *8*, 315 – 399; b) D. K. Chalmerst, G. R. Marshall, *J. Am. Chem. Soc.* **1995**, *117*, 5927 – 5937; c) J. Venkatraman, S. C. Shankaramma, P. Balaram, *Chem. Rev.* **2001**, *101*, 3131 – 3152; d) R. Rai, S. Raghothama, P. Balaram, *J. Am. Chem. Soc.* **2006**, *128*, 2675 – 2681.

[38] S. Hecht, I. Huc, *Foldamers: Structure, Properties and Applications*, Wiley, **2007**, p. 456.

[39] a) C. Toniolo, E. Benedetti, *CRC Crit. Rev. Biochem.* **1980**, *9*, 1 – 44; b) B. Imperiali, R. A. Moats, S. L. Fisher, T. J. Prins, *J. Am. Chem. Soc.* **1992**, *114*, 3182 – 3188; c) J. Yang, S. H. Gellman, *J. Am. Chem. Soc.* **1998**, *120*, 9090 – 9091; d) I. G. Jones, W. Jones, M. North, *J. Org. Chem.* **1998**, *63*, 1505 – 1513; e) L. Belvisi, C. Gennari, A. Mielgo, D. Potenza, C. Scolastico, *Eur. J. Org. Chem.* **1999**, 389 – 400.

[40] a) R. Kuroda, Y. Saito, in *Circular Dichroism: Principles and Applications* (Eds.: N. Berova, K. Nakanishi, R. Woody), Wiley-VCH, New York, **2000**, pp. 601 – 615; b) O. Pieroni, A. Fissi, R. M. Jain, V. S. Chauhan, *Biopolymers* **1996**, *38*, 97 – 108; c) A. Perczel, M. Hollosi, B. M. Foxman, G. D. Fasman, *J. Am. Chem. Soc.* **1991**, *113*, 9772 – 9784.

[41] M. Aschi, A. Mollica, G. Lucente, M. Paglialunga Paradisi, F. Mazza, *J. Mol. Struct.* **2006**, *785*, 176 – 181.

[42] R. Spadaccini, P. A. Temussi, *Cell. Mol. Life Sci.* **2001**, *58*, 1572 – 1582.

[43] K. Nguyen, M. Iskandar, D. L. Rabenstein, *J. Phys. Chem. B* **2010**, *114*, 3387 – 3392.

[44] K. Wüthrich, *NMR of Proteins and Nucleic Acids*, Wiley, New York, p. 320.

[45] W. D. Cornell, P. Cieplak, C. I. Bayly, I. R. Gould, K. M. Merz, D. M. Ferguson, D. C. Spellmeyer, T. Fox, J. W. Caldwell, P. A. Kollman, *J. Am. Chem. Soc.* **1995**, *117*, 5179 – 5197.

[46] G. Srinivasulu, S. K. Kumar, G. V. M. Sharma, A. C. Kunwar. *J. Org. Chem.* **2006**, 71, 8395 – 8400.

[47] P. Prabhakaran, S. K. Kale, V. G. Puranik, P. R. Rajamohanan, O. Chetina, J. A. K. Howard, H.-J. Hofmann, G. J. Sanjayan. *J. Am. Chem. Soc.* **2008**, *130*, 17743 – 17754.

[48] V. H. Thorat, T. S. Ingole, K. N. Vijayadas, R. V. Nair, S. S. Kale, V. V. E. Ramesh, H. C. Davis, P. Prabhakaran, R. G. Gonnade, R. L. Gawade, V. G. Puranik, P. R. Rajamohanan, G. J. Sanjayan, *Eur. J. Org. Chem.* **2013**, 3529 – 3542.

[49] G. V. M. Sharma, P. Nagendar, P. Jayaprakash, P. R. Krishna, K. V. S. Ramakrishna, A. C. Kunwar, *Angew. Chem.* **2005**, *117*, 6028 – 6032; *Angew. Chem. Int. Ed.* **2005**, *44*, 5878 – 5882.

[50] HyperChem, Release 8.0.3, Hypercube Inc., 1115 NW 4th St. Gainesville, FL 32608, USA, **2007**.

[51] M. P. Williamson, T. F. Havel, J. Wüthrich, *Mol. Biol.* **1985**, *182*, 295 – 315.

[52] W. L. Jorgensen, J. Chandrasekhar, J. Madura, R. W. Impey, M. L. Klein, *J. Chem. Phys.* **1983**, *79*, 926 – 935.

[53] H. J. C. Berendsen, J. P. M. Postma, W. F. van Gunsteren, A. Di Nola, J. R. Haak, *J. Chem. Phys.* **1984**, *81*, 3684 – 3690.

[54] W. Kohn, L. J. Sham, *Phys. Rev.* **1965**, *140*, A1133 – A1138.

[55] A. D. Becke, *J. Chem. Phys.* **1993**, *98*, 5648 – 5652.

[56] C. Lee, W. Yang, R. G. Parr, *Phys. Rev.* **1998**, *B37*, 785 – 789.

Received: March 8, 2014
Revised: July 7, 2014
Published online on September 2, 2014